Journal of Archaeological Science 77 (2017) 35–51

Contents lists available at ScienceDirect

Journal of Archaeological Science

journal homepage: http://www.elsevier.com/locate/jas

Marco Gonzalez, Ambergris Caye, Belize: A geoarchaeological record of ground raising associated with surface soil formation and the presence of a Dark Earth

Richard I. Macphail [a, *], Elizabeth Graham [a], John Crowther [b], Simon Turner [c]

[a] University College London, Institute of Archaeology, 31-34, Gordon Sq., London WC1H 0PY, UK
[b] Archaeological Services, Trinity St Davids, University of Wales, Lampeter, Ceredigion SA48 7ED, UK
[c] University College London, Environmental Change Research Centre, Gower Street, London WC1E 6BT, UK

ARTICLE INFO

Article history:
Received 28 August 2015
Received in revised form
25 March 2016
Accepted 8 June 2016
Available online 17 June 2016

Keywords:
Maya
Soil micromorphology
Chemistry
Floors
Salt working
Dark Earth
Mercury

ABSTRACT

Marco Gonzalez, on the south-west end of the island of Ambergris Caye, Belize, has well-preserved Maya archaeological stratigraphy dating from Preclassic times (ca. 300 B.C.) to the Late Classic period (ca. A.D. 550/600 to 700/760). Although later occupations are recorded by house platforms and inhumations (Terminal Classic to Early Postclassic), and use of the site continued until the 16th century A.D., intact stratigraphy is rare in these cases owing to a greater degree of disturbance. Nonetheless, understanding site formation entails accounting for all processes, including disturbance. The site's depositional sequence—as revealed through soil micromorphology and chemistry and detailed here—has yielded critical information in two spheres of research. As regards archaeology and the elucidation of Maya activities on the caye over time, soil micromorphology has contributed beyond measure to what we have been able to distinguish as material remains of cultural activity. Detailed descriptions of the nature of the material remains has in turn helped us to clarify or alter interpretations based on artefacts that have been identified or sediments characterised according to traditional recovery techniques. The other major sphere in which soil micromorphology and chemistry play a critical role is in assessment of the environmental impact of human activity, which enables us to construct and test hypotheses concerning how the site formed over time; what materials and elements contributed to the character of the sediments, especially in the formation of a specific Maya Dark Earth type that is developed from carbonate rich deposits; and how the modern surface soils acquired the appearance of a Dark Earth, but essentially differ from them. In terms of agricultural soil sustainability, the Marco Gonzalez surface soil is neo-formed by a woodland vegetation drawing upon the nutrients and constituents present in both the Dark Earth and underlying better preserved stratified deposits.

1. Introduction

A multi-disciplinary study of selected geoarchaeological and archaeological sequences was carried out at the Maya site of Marco Gonzalez, Ambergris Caye, Belize during 2013–2014 to investigate site formation processes. Understanding site formation is only one of a set of aims whose common properties are defined by our goal of elucidating the long-term role of human impact in the formation of the earth's cultivable soils (Graham et al., 2015). The content of this paper in particular is focused on describing the methods that we employed to sample, describe, analyse, and interpret all of the accessible strata that comprise the archaeological site. Our hope is that such methods—duplicated, altered, or improved—will be of utility to other researchers. Before describing the methods and results of the site formation research, and in order to contextualise the data and discussion presented here, we provide an outline of the cultural context and anthropological significance of the larger study, otherwise detailed extensively in other publications (Graham, 1998, 2006; Graham and Pendergast, 1992; Graham et al., 2015).

* Corresponding author.
E-mail addresses: r.macphail@ucl.ac.uk (R.I. Macphail), e.graham@ucl.ac.uk (E. Graham), simon.turner@ucl.ac.uk (S. Turner).

http://dx.doi.org/10.1016/j.jas.2016.06.003
0305-4403/

2. Site formation and its significance

One aim of characterising site formation processes, which is perhaps the original aim in archaeology, has been to contribute to a better understanding of the contexts for archaeological evidence (Schiffer, 1987). Soil micromorphological approaches have contributed inestimably to this aim at Marco Gonzalez. The results of soil micromorphological analyses have strengthened our hypothesis that salt production was an intensive economic activity at Marco Gonzalez in the Late Classic period (ca. A.D. 550 to 750). There are other instances, however, in which micromorphology has provided information on the origins of sediments that have yielded archaeological material, such as the Terminal Preclassic and Early Classic pottery in colluvial deposits sealed either by subsequent construction or by the debris of salt processing. Information on the material comprising the archaeological deposits—such as the ghost floors in the salt-processing debris and later habitation levels or the coprolitic bone material in the Early Classic levels—was simply not detectable by the naked eye during excavation. It should be noted that the soil micromorphological results, limited thus far to strata exposed in test pits, remain preliminary and much more extensive exposure will be required to gather evidence on the full range of occupational and processing activities at the site. However, the results described should nonetheless serve to demonstrate the ways in which our picture of the activities at the site has been clarified and enriched, and has helped us to develop a strategy for future research.

The other critical role of soil micromorphology is its contribution to our greater goal of assessing the environmental impact of human activity at Marco Gonzalez, which will enable us to construct and test hypotheses concerning how the site formed over time, what materials and elements contributed to the character of the sediments, and how the modern surface soils acquired the appearance of a Dark Earth (Graham et al., 2015). The dark brown to black surface soils, commonly removed by locals for use in their gardens, are typical of sites on the caye and of other sites in coastal Belize (Graham, 1994, 2006). They are shown, through the soil micromorphological analyses presented below, to be distinct from Amazonian Dark Earths (ADEs or *terra preta*) (Arroyo-Kalin, 2009, 2014; Arroyo-Kalin et al., 2009; Glaser and Birk, 2012; Glaser and Woods, 2004; Lehman et al., 2003; Sombroek, 1966; Woods et al., 2009), but they share critical characteristics, such as the ubiquitous presence of charcoal. Perhaps more important, Maya Dark Earth, like ADE, represents enrichment by activities for which humans were the catalyst. Dark earths have not received much attention in the Maya area, probably owing to the fact that evidence of the kind of enrichment documented for ADEs has been rare (Beach et al., 2015: 18). An initial study of soils at Marco Gonzalez (Beach et al., 2009) has, however, revealed a significant degree of enrichment, which supports the contention that studies of anthropogenic soils of Precolumbian origin should extend to areas of the Neotropics outside the Amazon (Arroyo-Kalin, 2014: 174; Graham, 2006).

We were able to build on an existing framework of the site's history, the result of excavations carried out in 1986, 1990 and 2010 (Graham and Pendergast, 1989; Graham and Simmons, 2012; Pendergast and Graham, 1987) (Fig. 1a). Our goal was to determine whether the sub-surface strata reflecting these sequences had contributed to the character of present-day soils and vegetation and, if so, to assess the nature of their contribution. Of major interest are the dark surface soils that are seemingly atypical compared to other Neotropical *terra preta* soils, known as Amazonian Dark Earths or ADEs (Arroyo-Kalin, 2014; Arroyo-Kalin et al., 2009; Graham, 2006). Accumulated remains of Maya occupation (mainly since ca. A.D. 100) including charcoal, pottery, and debris from hypothesised salt processing (A.D. 550/600 to 700/760) were investigated in detail. Development of the coast line, sea level change, mangrove formation, the modern day vegetation (Fig 2c), plant macrofossils, the site in its wider landscape and the results of Maya waste disposal in relationship to modern sustainable land use in the region were considered in addition to the geoarchaeological study presented here (Graham et al., 2015). This paper focuses on findings from the salt working levels, on the formation of a Maya Dark Earth, and on current surface soil development.

The island of Ambergris Caye is underlain by 'reefstone' (maximum elevation 1 m asl) of the Belize Barrier Reef, which formed >8.26 to 6.68 ky BP on Pleistocene reef limestones (Gischler and Hudson, 2004). Sea level rise since the Pleistocene has affected coastal morphology, with the shelf lagoon between the Belize Barrier Reef and the mainland already inundated by 5.6 ky BP; subsidence associated with fault-blocks below the reef has also occurred (Dunn and Mazzullo, 1993; Gischler and Hudson, 2004, 232–234; Gischler et al., 2000; James and Ginsburg, 1979). The site of Marco Gonzalez with its distinctive vegetation is easily spotted from the air at the southern end of the caye (Fig. 1c). At 3.5 m asl, it appears as a large mound surrounded by mangrove swamp and separated from the windward shores by beach sands. Research by Dunn and Mazzullo (1993) has shown that the site in the past was open to both the Caribbean and to the waters of the lagoon on the leeward side of the island. Preclassic deposits lie largely below the modern water table, but a sample of ceramics recovered from submerged strata indicate occupation at least by Late Preclassic times (ca. 300 BC- A.D.1), with intensification of marine resource exploitation and trading activity during the Terminal Preclassic period (ca. A.D. 1–250). Utilization of the site continued in various forms until early Spanish colonial times. The period that seems to have given the site the bulk of its modern configuration spans the end of the Late Classic to the Early Postclassic (ca. A.D. 760 to 1200). At the end of the Late Classic, sometime in the latter part of the 8th century A.D., a town of over 40 structures—reefstone platforms with perishable superstructures—was built. It is these structures that were mapped (Fig. 1b) and provide the loci for the excavation designations (e.g., Str. 1, Str. 22, etc.).

Our study sampled three locations: Str. 14 (Op 13–1), Str. 19 (Op 13–2) and Str. 8 (Op 13–3). The locations of Strs. 14 and 19 represent the highest elevations on site whereas Str. 8 lies at the (present-day) site periphery (Fig. 1b). No basal boundary between natural sediments and anthropogenic deposits was observed in thin-section samples (lowest sample at −0.23 m asl) because the earliest deposits lie below current high groundwater levels and were inaccessible. Earlier stratigraphic surveys by Dunn and Mazzullo (1993) propose that anthrosols sit, unconformably on a high shelf of Pleistocene limestone, which may preclude natural sediment being found at greater depth beneath the central area. Occupation detritus (sherds and conch) mixed with open marine sandy carbonate muds, estuarine mud/sand and mangrove sediments were found in cores to the south of the site in 2013. Artefact-containing sands and muds (extending >1.5 m below sea level) were recorded at the mangrove site margin (Graham et al., 2015), which suggests that a preserved boundary between natural sediments and earliest anthropogenic deposits can be found at selected locations.

3. Methods

Soil micromorphology focused on continuous and semi-continuous sequences and lateral control samples from the excavation units. Sampling extended from the excavated exposed 'surface' or modern topsoil, down to water-saturated levels at Structure 14, for example (−0.230–2.150 m asl); in addition, three further

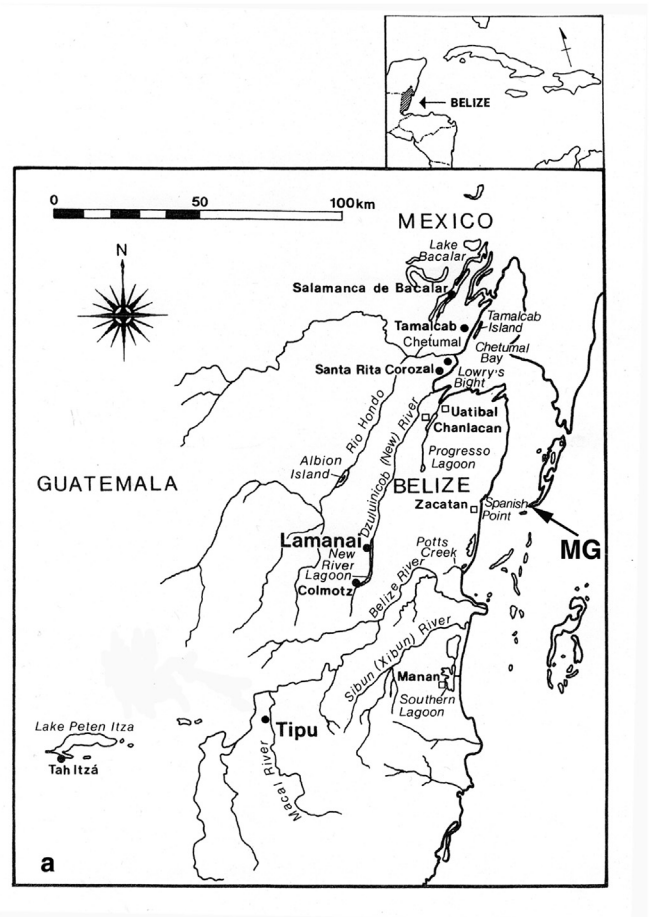

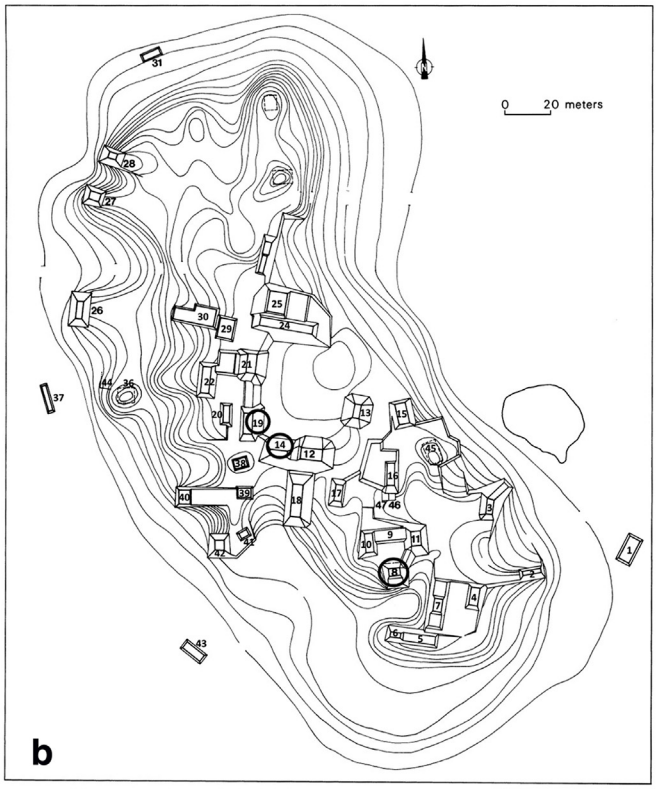

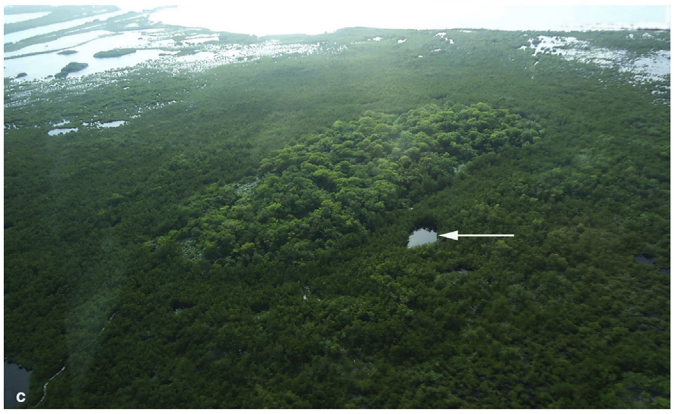

Fig. 1. 1a: Regional map showing location of Belize and Spanish Period sites; the island of Marco Gonzalez (MG) is at the southern end of Ambergris Caye; 1b: Marco Gonzalez – location of Structures 8 (Op 13-3), 14 (Op 13-1) and 19 (Op 13-2). Structures 8, 14 and 19 are ringed for clarity; 1c: Aerial photograph of Marco Gonzalez, looking south-west, showing broadleaved caye wooded island area within mangrove swamps. The 'small pool' which was cored, is arrowed; 1 d: Reconstructed cached Early Classic basal-flange bowl (390/1) found below lime plaster floors (see Fig. 2a).

surface soil locations were studied in thin section at Strs. 8, 19 and 25 (Fig. 1b). All monoliths (sampling vertical sections through excavated profiles) from Structures 8, 14 and 19 were sub-sampled for a suite of bulk analytical chemical, geophysical and particle-size techniques that had proven useful during investigations of intertidal, coastal salt making and European dark earth sites; European dark earth site-studies are thought to be relevant given the similar amount of lime-based plasters and limestone employed at Marco Gonzalez in comparison to Roman urban sites (Boorman et al., 2002; Borderie et al., 2014; Macphail, 2003; Macphail et al., 2010, 2012). A parallel series of bulk samples also underwent XRF and Hg analysis. The combined methods were selected to be consistent with those employed studying other Maya sites and Amazonian Dark Earths in general (Arroyo-Kalin, 2014; Arroyo-Kalin et al., 2009; Beach et al., 2006; Beach and Dunning, 1995).

Monoliths were examined and sub-sampled at the Institute of Archaeology, University College London by R. Macphail, so that selected bulk samples exactly matched thin section samples (online Table 1). Bulk soil analyses were carried out by J. Crowther at Trinity St David's, University of Wales, Lampeter; the same sample series underwent XRF and Hg analysis at the Department of Geography, UCL, by Simon Turner. All samples were freeze-dried, sieved at

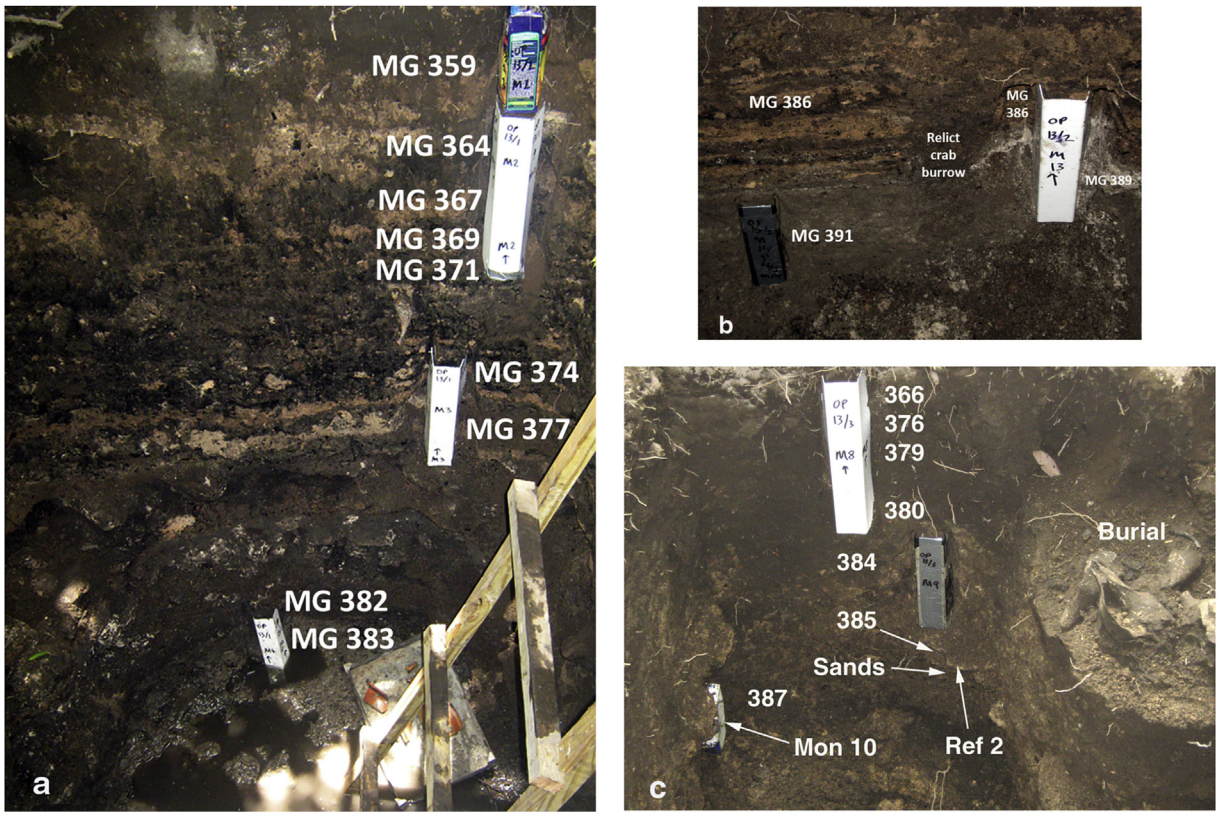

Fig. 2. 2a: Field photo of Op 13-1 (Str 14), east face, showing monolith samples 1–4 and MG Contexts: MG 359 ('Maya dark earth'); MG 364, 367, 369 and 371 (remains of weathering lime floors and salt processing residues and burrow-mixed 'Maya dark earth'; MG 374 and 377 (mainly intact lime floors and ash layers of salt processing origin); MG 382 (lime floors and trample, sealing cached Early Classic basal-flange bowls – see fragments on the board by the ladder and Fig. 1d); MG 383 (ash and fine bone-rich colluvium). On the west face, monoliths 5 and 7 sampled a lateral example of salt processing layers/floors (MG 377); monolith 6 sampled MG 383 to a depth of −0.230 m asl; 2b: Field photo of labelled Op 13-2 (Str 19). Lowermost monolith14 sampled MG 391 (waterlaid ashy colluvium and – upwards – a weathered soil surface); Monolith 13 also sampled this upper part of MG 391 and cemented ash layer MG 389 (see Fig. 3a); MG 386 is composed of a series of heated lime floors and burnt salt processing waste deposits. Overlying monoliths (not illustrated) sampled weathered lime floors and Maya dark earth (Monolith 12) and the surface soil (Monolith 11); 2c: Field photo of labelled Op 13-3 (Str 8) showing monoliths and Contexts. Monolith 8 sampled lime floor remains within 'Maya dark earth' (MG 366, 276 and 379) and weathered lime floor remains (MG 380) of the town. Monolith 9 also covered weathered lime floor remains (MG 384). A large lump of sediment from MG 385 (Ref 2) included an intact lime floor over 'sands' (see Fig. 5a–b). Monolith 10 sampled burrowed disturbed Late Classic deposits, which also included a thick intact ash layer (MG 387).

<125 μm and homogenised for measurement of Hg and XRF analysis.

Subsampling for bulk samples and resin-impregnation of intact monolith material for thin section production followed established protocols (Goldberg and Macphail, 2006). Bulk analyses involved the testing of 39 samples for organic matter (LOI: loss-on-ignition), carbonate (LOI @ 950 °C), fractionated P, pH, specific conductance ('salinity') and magnetic susceptibility (χ, χ_{max} and $\%\chi_{conv}$), with 10 samples also being analysed for particle size (Avery and Bascomb, 1974; Scollar et al., 1990; Tite, 1972; Tite and Mullins, 1971). LOI (organic matter) and carbonate content were determined by sequential ignition: at 375 °C for 16 h (Ball, 1964) – previous experimental studies having shown that there is normally no significant breakdown of carbonate at this temperature – and at 950 °C for 2 h; for a separate surface soil mapping study carried out at UCL a temperature of 550 °C for 2 h was employed (Heiri et al., 2001). Phosphate-Pi (inorganic phosphate) and phosphate-Po (organic phosphate) were determined using a two-stage adaptation of the procedure developed by Dick and Tabatabai (1977) in which the phosphate concentration of a sample is measured first without oxidation of organic matter (Pi), using 1 N HCl as the extractant; and then on the residue following alkaline oxidation with sodium hypobromite (Po), using 1 N H_2SO_4 as the extractant. Phosphate-P (total phosphate) has been derived as the sum of phosphate-Pi and phosphate-Po, and the percentages of inorganic and organic phosphate calculated (i.e. phosphate-Pi:P and phosphate-Po:P, respectively). Mercury (Hg) analyses employed cold vapour-atomic fluorescence spectrometry (CV-AFS) at UCL.

Out of a total of 44 thin-sections studied, SEM/EDS (Energy Dispersive X-Ray Spectrometry; Weiner, 2010) was carried out on specific features in 7 thin sections. Thin sections were described, ascribed soil microfabric types (MFTs) and microfacies types (MFTs), and counted according to established methods (Bullock et al., 1985; Courty, 2001; Courty et al., 1989; Macphail and Cruise, 2001; Stoops, 2003; Stoops et al., 2010).

4. Results and preliminary discussion

Results are presented online in Tables 2–5 and illustrated in various thin-section scans, photomicrographs and a SEM X-Ray backscatter example. Presentation of our overall methodology and its effectiveness in light of preliminary results has been published (Graham et al., 2015). The following sections assess our understanding of deposit accumulation and its significance in relationship to Dark Earth and surface soil formation (Table 1).

4.1. Preliminary results from surface soils and off-site sediment sequences

Subsamples from the micromorphology sections show that

Table 1
Summary of soil micromorphology and bulk soil findings – both generalised and Context-specific.

Contexts/ structures	Soil micromorphology and bulk soil data interpretations	Period and further information
Surface soil Litter (L) and Ah1 horizon Op 13/2-3 (Str.19 and 8) and Structure 25	Most organic (highest LOI) and mercury (Hg)-rich, and least alkaline layer, with biologically mixed humic mineral soil and litter (L) layer of typical Mull humus horizon, which is granular to extremely fine pellety in character. Preliminary findings from ongoing research suggest that elevated mercury, adsorbed to organic matter, is owing to surface soil accumulation from the underlying anthropogenic deposits – drawing on natural marine Hg accumulators (large reef fish residues?). Relatively high phosphate levels may result from relict bone and possible effects of decomposition of inhumations (also likely influencing character of dark earth). Litter includes horizontally oriented leaves and extremely thin organic excrements (of Oribatids?) and broad organic excrements composed of finely comminuted plant fragments; aggregated amorphous organic matter produced in this Litter layer forms broad excrements (granules/crumbs) which embed fine mineral grains and remains of lime floors, shell and reefstone fossils. Fauna include land snails and amorphous organic matter which is probably part remains of termite nests (which have also contributed to reference thin sections). Unlike the dark earth, these surface soils and litter layers include very little fine or very fine charcoal and testify to surface accumulation and mixing of organic matter from inputs of plant litter, roots and termite nest materials – possibly over the last 50–100 years. The plants at the site have recycled chemicals including mercury, iron and probably phosphate into the organic matter from the underlying anthropogenic deposits. In addition, as carbonate-rich residual materials were decalcified, phosphate-rich material – bone and mineralised coprolitic material – would have been relatively concentrated, while plant humus accumulation concentrated mercury.	*Modern* Vegetation survey (R. Whittet and C. Rosique in Graham et al., 2015) found that the mangrove-girt island has an interestingly rich flora (64 species) with a wooded central part broadly consistent with "Caye Forest" and "Caye Broadleaved Forest" classifications, and with salt-tolerant plants on its margins and some few patches of recently introduced species (e.g. *Cocos sp.*). Land crab activity/burrowing in evidence at lower elevations (Glanville-Wallis, 2015); hermit crab use of ancient conch shells.
Dark earth Op 13/1–3 (Str. 14, 19 and 8) Op 13/3 (Str. 8) Context 379	Typified by total biological microfabrics of very fine charcoal-rich soil – hence dark colour – containing relict clasts of resistant burned sediment, ash nodules and calcined bone, for example, while lime plaster floors and fragments show dissolution and sometimes recrystallization of calcite (micrite), and can occur as 'ghost' layers. Leaching has caused marked reduction specific conductance (salinity) and progressive decrease in carbonate content; phosphate however can increase up-profile. Also Hg-rich when burrow-mixed with humic surface soils. Essentially recemented ghost of lime plaster floor(s) within 'dark earth' and showing calcitic root pseudomorphs of weathering history. Upwards there are only finely fragmented gravel-size floor remains, with a marked modern total biological microfabric, and increased humic content (LOI) and phosphate in a broad burrow/feature fill (grave?) that is also currently rooted. Upwards (Contexts MG 366 and 376) relict and fragmented lime plaster floor soil is increasingly mixed with more humic and very fine charcoal-rich soil – including humic peds worked down from modern surface soil. Within this dark earth, however, there was *in situ* deposition of faecal waste – either of human or possibly pig origin, recording post-town Postclassic and later/colonial occupation (?).	Town established in Late Classic to Terminal Classic times (late 8th to early 9th century) and occupied into the Early Postclassic (ca. AD 1200/1250); structures of this period are characterised by numerous sub-floor burials. Less intensive use of the site after the Early Postclassic but residential and ritual activity continues through to the Contact period (1500s). The town was built over stratified salt processing debris that dates largely to the Late Classic (ca AD 600–750). Land crabs are active throughout these periods where the water table is more easily accessible, i.e. at low elevations.
Op 13/3 (Str. 8) Context 380 Context 384 Context Upper 385	Weathered and biologically burrowed soil formed in lime plaster floor remains, with semi-intact layers present; minor increased amounts of organic matter and slightly less carbonate are consistent with nearer surface weathering, while increased phosphate may be of both settlement and settlement-associated burial origin; upwards, more humic and totally biologically worked dark earth soil. Diffusely and broadly layered ca. 10–15 mm thick remains of decalcified lime floor and moderately intact lime floor remains (burnt shell remains suggest continued use of burnt shell as a lime source); less evidence of use of tidal flat clays as temper/addition compared to salt processing levels and earlier. Domestic lime floor over marine sands (marine inundation high point at 0.37 m asl).	No primary dating from this structure; estimated from ceramics to date from the Late/Terminal Classic to Early Postclassic (see above). Sub-floor burials present but heavily disturbed; extensive disturbance by land crabs has mixed Late Classic salt processing (AD 600–750) with later floors associated with Str. 8.
Op 13/1 (Str. 14) Contexts 359-377 and Structure 19 Context 386 Op 13/3 (Str. 8) Context 385 Context 387	Salt working deposits formed: a) little disturbed and sometimes totally *in situ* ashy combustion zones, b) *in situ* lime plaster floors, c) chaotically mixed burned marine sediment clast layers (with high specific conductance and magnetic susceptibility), with various proportions of ash and coarse charcoal present, and d) occasional trampled occupation surfaces showing minor weathering features and bone-rich kitchen midden waste; presence of shells which had 'trapped' fossiliferous beach sands. Findings suggest use of tidal flat sediments (probably periodically exposed environment) for source of naturally concentrated salt, which when mixed with sea water produces brine; this was heated on small low- temperature fires located on lime plaster floors which acted as the hearth base. Mainly	Late Classic salt processing (AD 550/600 to 700/760) contexts High concentrations of crudely made, roughly standardised quartz sand-tempered pottery vessels (Coconut Walk ware) for holding brine; fuel waste wood charcoal alos present; quartz sand not local to island (Graham et al., 2015); some evidence of crab burrows.

(*continued on next page*)

Table 1 (*continued*)

Contexts/ structures	Soil micromorphology and bulk soil data interpretations	Period and further information
	siliceous fossil (sponge spicule)-rich fine tidal flat sediment was employed – as also found coating quartz sand-tempered Coconut Walk pottery fragments. Some mollusc shells, once processed for food, and which were discarded on the beach, were sometimes recycled for constructions or lime burning. 15-20 mm-thick lime floor (with decalcified weathered upper surface) was constructed on medium to coarse and fine to medium upward-fining beach sands at 0.39 m asl. This indicates a Late Classic marine inundation event (storm surge?). Burrowed and finely fragmented remains of weakly rubefied lime plaster floors, burned clay, ash and charcoal; loose fine charcoal coats plaster and ash clasts; 35 mm-thick intact partially 'cemented' ash layer survives within burrowed zone.	
Op 13/1 (Str.14) Context 382 Op 13/2 (Str. 19) Contexts 389-386	Construction of a series of lime plaster floors (for example over a cached Early Classic bowl), tempered with isotropic siliceous microfossil (sponge spicule)-rich tidal flat sediment clasts of various sizes (silt to gravel size), and incorporating charcoal and fine burned bone, with pure micritic lime plastered surfaces, conceivably of ash (?) origin. Upwards, 391 is sealed by a series of ash layers (389–386) – some 'wetted' and recemented – with an interbedded series of thin, trampled deposits, which can be extremely rich in heated/burned bone (mainly fish bone) and record the highest phosphate content at Marco-Gonzalez. In this 'domestic' occupation area, these are presumed fireplaces used for food preparation which may have included low temperature cooking/smoking of fish.	Early Classic occupation (AD 250–550/600) Macrofossils of maize (*Zea mays*) and craboo (*Byrsonima sp.*); their presence is indicative of trade (L. Duncan in Graham et al., 2015).
Op 13/1 (Str. 14) Context 383 and Op 13/2 (Str. 19) Context 391 (389?)	Rainstorm erosion of putative ash-rich hearths/ash dumps, with associated burned bone (cooking), heated bone (low temperature cooking - food processing – smoking?) and possible human waste (coprolitic bone?), all including fish bone, producing waterlaid ashy sediments in low ground. High-energy colluviation resulted in coarse lens composed of gravel-size lime plaster, potsherds, bone, bioclastic limestone and charcoal. Exposure and short period of stasis led to weak weathering effects and biological working of the uppermost sediments at both locations. At Structure 19 these sediments were composed of shell- and bone-rich kitchen midden deposits at the top of Context MG 391. Anthropogenic nature of waterlaid sediments implies high occupation concentrations upslope.	Terminal Preclassic intensive occupation (ca. AD 100–250?) Coring data suggest the presence of such 'early' ash-rich sediments on the now-mangrove covered margins of the island (see S. Turner in Graham et al., 2015). Macrofossils of maize (*Zea mays*) and craboo (*Byrsonima* sp.) are indicative of trade/exchange (L. Duncan in Graham et al., 2015).

there is a strong association of Hg with surface humic horizons, compared to units found at depth. Other metals (Ni, Cu, Zn and Pb; online Table 2) often associated with usage and human activities do not show the same affinity. These findings indicate that the locations of the occupation and processing units we sampled are not associated with sites of intensive metal processing or waste disposal (e.g. Cook et al., 2006). Instead, a mechanism of Hg surface enrichment has operated, seemingly alongside the post-occupation development of soils at the site. How enhanced a process this has been and whether the association with human activity at Marco Gonzalez is causal remains to be investigated. It is noteworthy that the topsoil value of Hg in OP13/3 (467.5 ng g^{-1}) is comparable to values (491 ng g^{-1}, $n = 30$, range 100–1718) found in London, UK (Yang et al., 2009).

Measurement of Hg and other geochemical variables in surface soil samples at the site is in progress in order to determine whether surface enrichment of Hg is related to proximity to structures, and/or whether other spatial variables such as altitude, soil organic content and vegetation patterns are significant. Similar measurements of geochemical variables in the off-site core sequences are ongoing, to investigate whether or not the timing of enrichment is linked to the occupation or post-occupation periods.

Preliminary analysis of diatom remains found in a core collected from the pool to the south-east of the site (Fig. 1c), has found that sponge spicules (*Placospongia* sp. and *Chondrosida* sp.) are abundant in deeper carbonate sandy muds, suggestive of reef back-barrier intertidal muds. Diatoms indicative of mudflat/estuarine conditions (e.g. *Navicula peregrina*, *Mastogloia lanceolata*, *Petroneis granulata*, *Surirella fastuosa*) are preserved with the transition to fine grain, more organic and non-carbonate muds (contemporaneous with shallowing of the water around the site), while sponge spicules disappear. The robustness of sponge spicules to post-burial dissolution compared to diatom valves may have contributed to the concentrated presence of sponge spicules at the base of the pool sequence but not to their decline further up in the core sample. Their reduction in frequency upwards in the sediment therefore likely relates to a reduction of local sponge habitat due to shallowing (mangrove development) and excessive sedimentation (Bell et al., 2015) during the later occupation of the island. This finding is important because, as discussed below, clasts of sponge spicule-rich clayey sediment, of presumed local off-site origin, occur as temper within lime plaster floors and as burnt residues in the processing deposits. The same sediment seems also to be present as intact coatings on sherds of a particular type of ceramics ('Coconut Walk unslipped', discussed below).

4.2. Bulk soil analyses

Data are presented in online Tables 2–4 *Particle size* analysis proved problematic owing to the large quantities of carbonate present (online Table 3). Only the surface soil from Op 13/3 (Str. 8) and sample × 13c at Op 13/2 (Str. 19) stand out as having rather more substantial and coarser carbonate-free sand fractions (~14–16% sand). As natural quartz sand is rare at the site, and often only seen in pottery sherds (Aimers et al., 2016), any non-calcareous sand concentrations could be regarded as mainly anthropogenic in origin – e.g. pottery disaggregation in surface soils. Soil micromorphology shows that much of the acid-insoluble

silt and clay is probably of locally imported non-calcareous fine sediment origin employed as temper fragments in plaster floors and as an industrial raw material in salt working (see below). *LOI* – which reflects a combination of soil organic matter and/or charcoal in the contexts analysed, displays very marked variability (range: 2.02–28.1%). As would be expected, the highest values were recorded in the two surface soil samples, from Structures 8 (LOI, 28.1%) and 19 (26.9%). In both these samples high values appear to be attributable to a high soil organic matter content, rather than the presence of large amounts of charcoal, as confirmed by soil micromorphology (see below). This being the case, it should be noted that these surface soils are particularly organic-rich, suggesting either that they have been enriched through anthropogenic activity or that organic decomposition is inhibited by poorly-drained conditions. (In fact, minor waterlogging microfeatures such as plant ferruginisation were noted in thin section, and no artificial additions were in evidence). These surface soil characteristics– as detailed further from the soil micromorphology (Fig. 6a–d) – are likely linked to the current vegetation cover, and other chemical measurements (Hg, specific conductance, pH, and carbonate content; see Table 1) that help differentiate these soils from ADEs. *Phosphate-P* concentrations are highly variable, with some samples exceptionally enriched, and phosphate being very dominantly inorganic (80->90% inorganic P). At the lower end, 19 samples have concentrations in the range 1.09–4.50 mg g^{-1}; soil micromorphology indicates that these are often layers rich in burnt intertidal sediment fragments. The remaining 20 samples, which have concentrations of 5.42–36.5 mg g^{-1}, are therefore interpreted as displaying phosphate enrichment to very strong enrichment (online Table 2).

All samples contain high or very high proportions of *carbonate* (range: 33.5–75.0%), with the majority containing $\geq$ 50.0%. All samples analysed also display very marked variability in *specific conductance* ('salinity'). Two of the lowest values were recorded in the two surface soil samples from Structures 8 and 19, with values of 455 and 477 μS, respectively. The values suggest that the upper horizon of the soils is subject to some degree of leaching. The majority of the samples, in contrast, are much more saline ($\geq$2500 μS), with seven having values $\geq$ 5000 μS (maximum: 5700 μS). Although it seems likely, in this near-coastal environment, that the salts are largely of natural origin (saline groundwater), it should be noted that six of the seven samples with the highest salinity levels contain ash, charcoal and/or burnt residues, and are apparently out of reach of saline ground water. Given these findings, *pH* analyses found that the samples are all alkaline, with expectable pH values ranging from 7.9 to 9.1. The lowest values were recorded for the two surface soil samples from Structures 8 and 19 (7.9 and 8.0, respectively), which is consistent with their notably lower carbonate content and salinity.

Magnetic susceptibility analyses demonstrated that the χ values are extremely variable, ranging from 4.8–641 $\times$ 10^{-8} m^3 kg^{-1}. Unusually, the χ_{max} values exhibit a similar range (14.8–714 $\times$ 10^{-8} m^3 kg^{-1}) and the resulting χ_{conv} values are exceptionally high ($\geq$37.4%), with nine samples having values $\geq$ 100.0% (i.e. $\chi \geq \chi_{max}$). These findings are anomalous, but have been encountered before in the study of three tropical African and Mediterranean sites (Crowther, 2014). Thus these data need to be treated with caution. In the specific case of the deposits at Marco Gonzalez where there are burnt ferruginous sediment inclusions, it has been argued that the combined effects of 1) fermentation in exposed tidal mudflats (see below), where enhancement potential could become naturally close to 'saturation', and 2) the burning of such sediments (where they are found as inclusions within lime plaster floors and within the Late Classic processing deposits) may be responsible for these anomalously high values (Graham et al., 2015). In short, the suggested strong effects of fermentation may therefore make indications of heating/burning less evident in both χ and χ_{conv} data. LOI, carbonate, phosphate, specific conductance (salinity) and magnetic susceptibility data are discussed later in relationship to soil micromorphology and context.

5. Soil micromorphology and discussion

Some sixty microstratigraphic layers were described and counted, with one thin section, for example, having 6 units composed of lime plaster floors and use deposits; a number of soil micromorphological descriptions and identifications are complemented by EDS data (online Table 5). The layers are described according to the activities they represent, in chronological order (see Table 1 for summary).

1. Terminal Preclassic (AD 1–250)/Early Classic (AD 250–550/600) settlement activities and island morphology development,
2. Early Classic lime plaster floor constructions (AD 250–550/600),
3. Late Classic intensive processing and associated occupation features (AD 550/600–700/760)
4. A poorly dated Late Classic or possibly later depositional sequence at Op 13-3 (Str. 8) – example of intact weathered lime floor over sands of inundation origin within generally burial and burrow-disturbed stratigraphy.
5. Terminal Classic (AD 760/800-AD 950/1000) to Early Postclassic (AD 1000–1250) town, and probable beginning of major deposit weathering and dark earth formation during the less well documented Contact and Colonial Period, with periodic habitation and use until the end of the 16th century and until quite recent times,
6. The modern surface soil and vegetation – the ages of which are unknown although the current vegetation is possibly only of 50–100 years in age.

5.1. Terminal Preclassic (AD 1–250)/Early Classic (AD 250–550/600) settlement activities and landscape development

The lowermost sediments—that is, the lowermost accessible deposits before groundwater made sample recovery impossible—as sampled in Op 13–1, Str. 14 (MG 383) (Figs. 1b and 2a) are composed of microlaminated (or burrow homogenised) compact calcitic ash in which there are very abundant small bone inclusions; many inclusions are fish bones, including vertebrae. Notably, in Op 13-2, Str. 19 (MG 391) (Fig. 2b), a very similar sediment type is present. At both locations, some bones are pale yellow to almost colourless and are probably poorly preserved ('partly digested/leached') assumed coprolitic bone, whereas orange-coloured and white calcined bones were probably heated and burned, respectively (Macphail and Goldberg, 2010). EDS analyses (M4D, MG 383) indicate that coprolitic bones are depleted in Ca and P compared to burnt bone (coprolitic bone: Ca = 36.6–37.7%, P = 15.6–17.5%; burnt bone: Ca = 39.0–39.3%, P = 17.1–18.7%; online Table 5). The amount of bone overall is consistent with Contexts MG 383 and MG 391 having some of the highest phosphate concentrations at Marco-Gonzalez (×13 b-14 d: 22.5–28.1 mg g^{-1} phosphate-P, n = 7; online Tables 1–2). As two areas of the ashy matrix material were found by EDS to contain 1.99–3.36% P, phosphate in general could have been 'fixed' in this calcareous environment, where phosphate is 98.6–99.0% in its inorganic form. It is considered that MG 383 and MG 391 are waterlaid colluvial sediments (Graham et al., 2015).

The presence of waterlaid and now waterlogged sediments is consistent with suggested lower base levels during the initial Maya

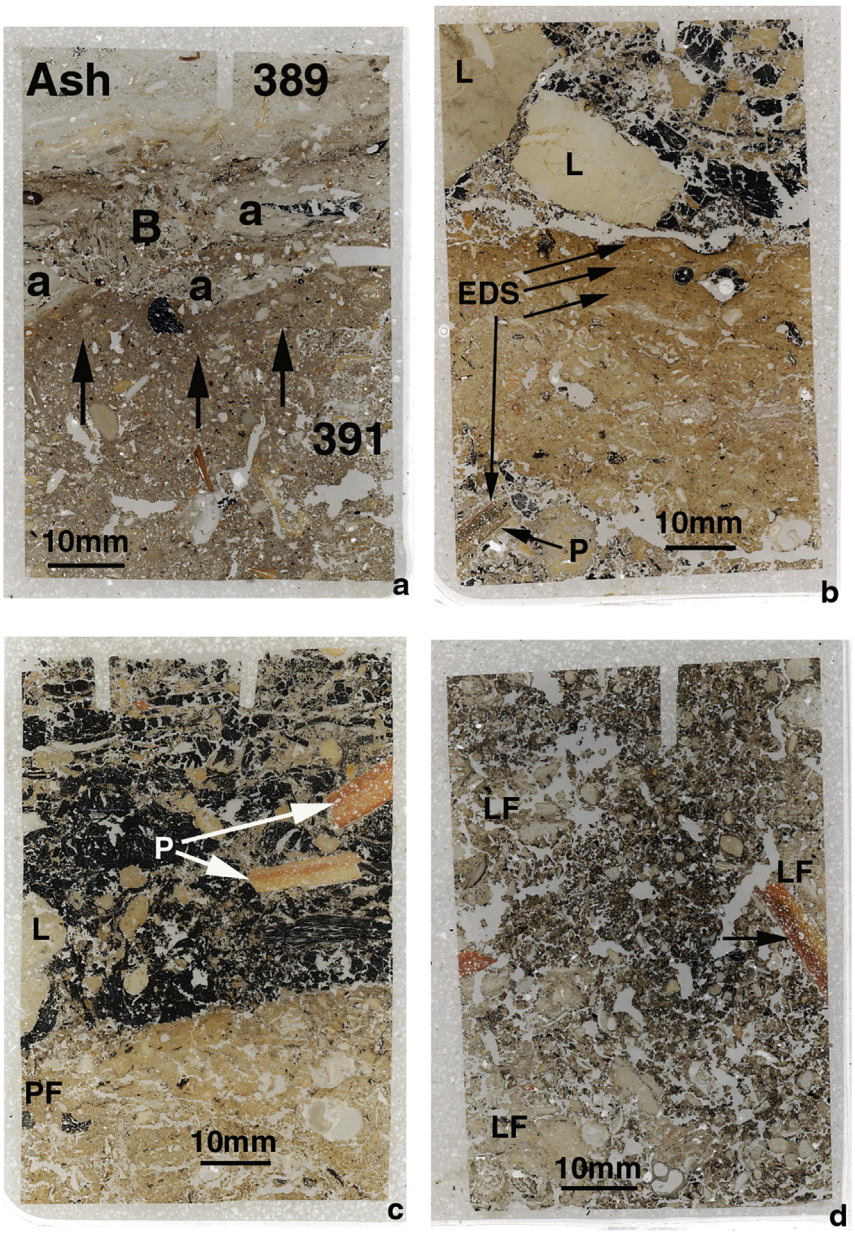

Fig. 3. 3a: Flatbed scan of thin section of M13D; junction of Contexts MG 391 and 389 (see Fig. 2a). A weathered and bioworked surface soil (391 – arrows) in ash and bone rich Early Classic deposits and the overlying massive ash layers from Late Classic occupation and salt processing. Lower ash layers (a) have been fragmented by burrowing (B). Scale bar = 10 mm; 3b: Flatbed scan of thin section M3B (Str 14, Op 13-1; west face); here a Late Classic heated lime plaster floor is overlain by chaotic dump of coarse limestone clasts (L), charcoal (fuel residues) and pink coloured plaster and sediment fragments, including isotropic sediment containing sponge spicules. The floor also seals a loose deposit that includes a sediment-coated Coconut Walk ware potsherd (P). Energy dispersive X-Ray spectrometry (EDS) studies were carried out on pot examples and the plaster floor (EDS) (see Fig. 4e and online Table 5). Scale bar = 10 mm; 3c: Flatbed scan of thin section M7A (MG 377; Str 14, other side (east face) of sondage Op 13-1); Late Classic salt working levels composed of a chaotic mixture of ash, charcoal, limestone (L), pink fragments of lime plaster floor and burnt sediment, and including two fragments of sediment-coated Coconut Walk ware potsherd (P), over intact lime plaster floor (PF). Scale bar = 10 mm; 3d: Flatbed scan of M2A (Str 14, Op 13-1; west face; uppermost MG 364); weathering lime plaster floor fragments (LF) in 'Maya dark earth' – here shown as a very broad burrow fill of dark soil composed of thin and broad organo-mineral excrements from invertebrate soil mesofauna activity. Note use of potsherd as temper in floor plaster (arrow). Scale bar = 10 mm. (For interpretation of the references to colour in this figure legend, the reader is referred to the web version of this article.)

occupation of the island, with subsequent rise in sea level (Dunn and Mazzullo, 1993) – see Op 13-3 for inundation event. The sediments also record Terminal Preclassic activities which produced large amounts of ash and bone. Such deposits were subsequently eroded, with ensuing colluviation infilling low ground within and around the areas of occupation and into the proximal estuarine/developing mangrove site margins; the last was indicated by Turner's borehole studies.

At both Op 13-1 (Str. 14) and Op 13-2 (Str, 19) the waterlaid ash sediments were biologically worked, marking a period of exposure and minor weathering ('soil ripening'). Whereas in Op 13-1 the biologically worked surface was sealed by a series of lime plaster floors (see below—dated to the Early Classic), in Op 13-2, the uppermost biologically worked ashy 'soils' record midden remains (uppermost MG 391) sealed by *in situ* ash layers (MG 389; Figs. 3a and 4a). Here (MG 389; M13D), there is a 200 mm-thick series of compact ash and trampled occupation floor layers, which continue upwards through M13B (MG 389-386) that are extremely rich in

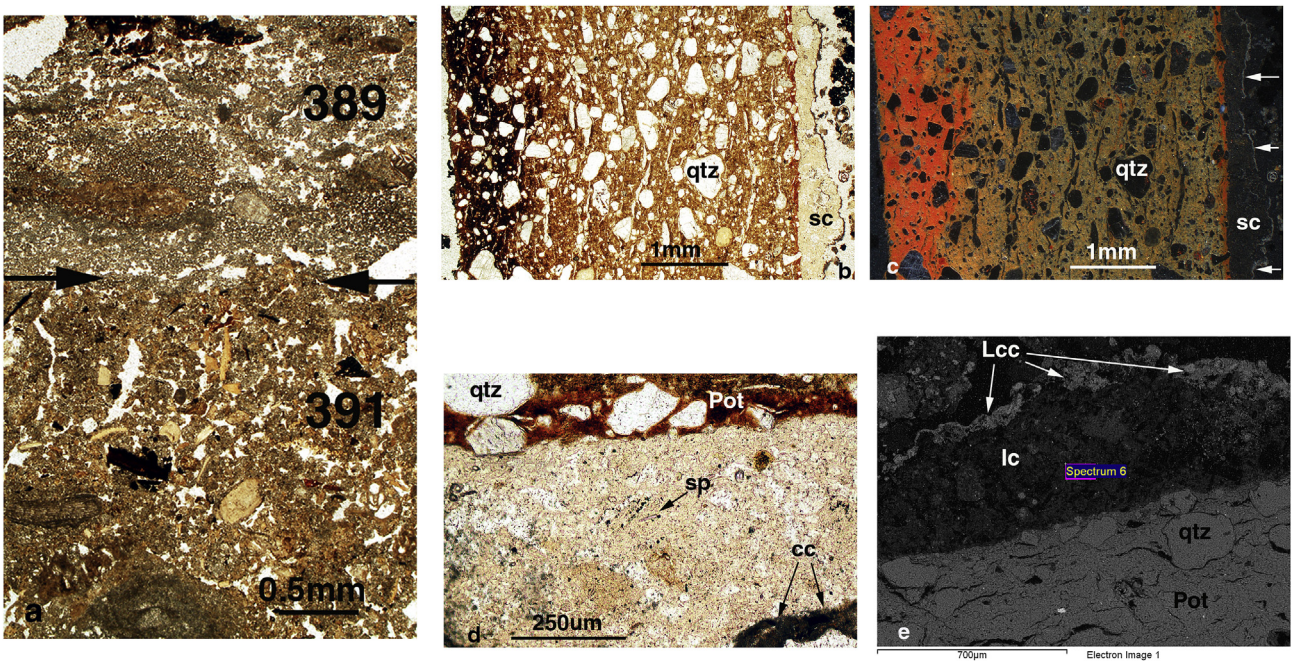

Fig. 4. 4a: Photomicrograph M13D detailing the junction between MG 391 and 389 (arrows; see Fig. 3a); *in situ* calcitic ash and laminae of cemented ash crystals in MG 389 were deposited over the bioworked and humic stained, bone and ash rich middening deposits of MG 391 where a soil had begun to develop. Plane polarised light (PPL), scale bar = 0.5 mm; 4b: Photomicrograph of M3A; isotropic sediment-coated (sc) Late Classic Coconut Walk ware potsherd tempered with quartz sand (qtz); quartz sand is not natural to the site (see Fig. 4c–e). PPL. Scale bar = 1 mm; 4c: As Fig. 4b, under oblique incident light (OIL); isotropic sediment coating is iron-depleted (colourless); background calcitic is arrowed. Scale bar = 10 mm; 4d: As Fig. 4b – detail of isotropic sediment pot coating. Coconut Walk ware pot is quartz sand-tempered. The sediment coating is siliceous and includes sponge spicules (sp), and is of exactly the same character as the burnt clay clasts present in the chaotic dumps of salt working waste (see Fig. 4e). This sediment is strongly attached and is regarded as recording the sea water-sediment mixture (brine concentration) which was heated to produce salt. Background calcitic debris loosely coats this attached isotropic coating (arrows). PPL. Scale bar = 250 µm; 4e: SEM X-Ray backscatter image of M3a (MG 374) – junction of Coconut Walk ware potsherd (Pot) tempered with quartz sand (qtz) and isotropic sediment coating (Ic) and location of one Spectrum. Note loose calcitic coating (Lcc) derived from the background ashy deposit. Scale bar = 700 µm.

heated and more strongly burnt fish bones that are often horizontally oriented. This amount of bone is consistent with the highest phosphate measurement at the site, for example (×13b – 36.5 mg g^{-1} phosphate-P). This may be showing renewed occupation associated with processing activity that produced large amounts of fuel ash in the Late Classic Period (MG 389-386; ca. 550-760 AD). (Conjecturally, salt processing deposits raised the occupation surface above water.

At Op 13-1 (Str 14) constructed lime plaster floors (base of MG 382) stratigraphically sealed two cached Early Classic basal-flange bowls (MG 390) (Fig. 1d). A series of fragmented, but still horizontally oriented lime floors occur alongside their intercalated trampled floor use deposits (Graham et al., 2015). Of particular interest is the use of specific kind of clay clasts as temper within the lime plaster binder. These are isotropic, siliceous in character, and include sponge spicules, and are believed to originate from intertidal/back reef mudflat sediments that are non-calcareous (see Late Classic deposits and plaster floors; EDS online Table 5: M3A, M3B, M7B). It is conceivable that this addition made the floors stronger; suggested Maya pozzolanic plasters employing volcanic inclusions have been reported from inland Belize (Villaseñor and Graham, 2010).

5.2. Late Classic intensive processing and associated occupation features (AD 550/600–700/760)

In Op 13-1, Str. 14, the layers reflecting intensive (salt?) processing were examined from ~2.075–1.070 m asl (MG 359-377) on the east face above the masonry platform (MG 382) (Figs. 2a, 3b–c). On the west face, the same layers (Monolith 7) had subsided into a gap within this rock platform (Monolith 5) so that they extended downwards to 0.530 m asl (MG 377 within MG 382). At Op13-2, Str. 19, this period is represented by deposits between 1.130 and 0.870 m asl (MG 386 and 389; see Figs. 3a and 4a), while mainly only strongly disturbed deposits occur at Op 13-3 (Str. 8) at 0.350–0.170 m asl (Fig. 2b–c). A range of layer types can be described, however. As described in Graham et al. (2015), these are:

a) little disturbed and sometimes totally *in situ* ashy combustion zones,
b) *in situ* lime plaster floors (Fig. 3b–c),
c) chaotically mixed burned sediment clast layers, with various proportions of ash, coarse charcoal and Coconut Walk ware sherds present (Figs. 3b–c, 4b–e), and
d) trampled occupation surfaces showing minor weathering features and bone-rich kitchen midden waste.

Here, we will only highlight new EDS and microfossil investigations of these facies types.

a) Totally in situ ashy combustion zones. These ashy hearth/combustion zone layers, including massive cemented ash and little-weathered ash layers, also display horizontal ash layers thinly interbedded with charcoal (*in situ* hearths). For example, at the base of MG 374, small *in situ* fires with 0.5–1.5 mm-thick ash and charcoal layers are present; it is suggested that these represent fuel layers that were originally ~75–225 mm thick (Courty et al., 1989). One such series of small fires reddened (rubefied) the uppermost 15 mm of the 40 mm-thick lime plaster floor that capped MG 377 (Fig. 3b–c) (see below). Such small fires would have produced low-temperature heating consistent with boiling brine (Biddulph et al., 2012).

b) In situ lime plaster floors and constructed surfaces An extensive

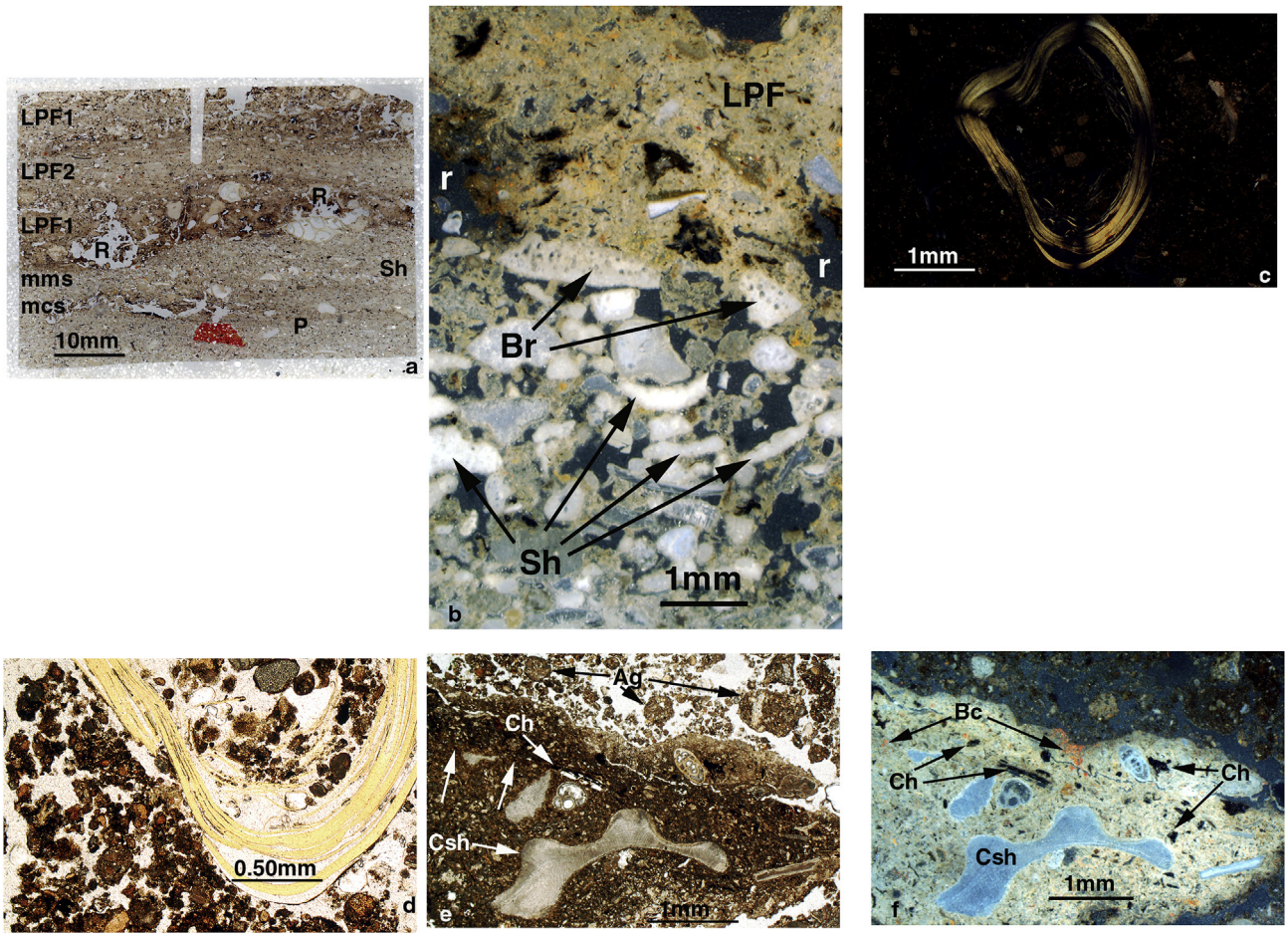

Fig. 5. 5a: Flatbed scan of MG Ref 2 (Str 8; Op 13-3; see Fig. 2c); Late/Terminal Classic to Early Postclassic (see Table 1) intact lime plaster floor and underlying sands (see Fig. 5b). Sands (beach sands?) are upward-fining calcareous fossiliferous mainly medium sands (mms) over mainly coarse sands (mcs) and gravels, and which include a pot fragment (P). At the top of the sands/base of lime plaster floor there is a gastropod (conch?) shell fragment (Sh). Lime plaster floor appears to be composed of at least 3–4 layers (LPF). Layer 1 shows organic staining and root channel-dissolution (R). Although looking similar in this scan, Layer 3 – which is the upper surface – is more decalcified and decarbonated compared to underlying Layer 2. This is due to soil leaching. Scale bar = 10 mm; 5b: Photomicrograph of MG Ref 2 (Str 8; Op 13-3; see Fig. 5a); junction lime plaster floor (FPF) and underlying fossiliferous and calcareous beach (?) sands containing bryozoan reef limestone/reefstone (Br) and shell (Sh). Here marine inundation occurred at 0.35 m asl over Late Classic salt working deposits (see Fig. 2c). Note dissolution of plaster floor in root channels (r). Oblique incident light (OIL). Scale bar = 1 mm; 5c: Photomicrograph of M1A (Str 14, Op 13-1; west face; MG 359); section through EDS-studied unknown/presumed plant root within pellety 'Maya dark earth' soil (see online Table 5), which shows moderate interference colours consistent with the presence of cellulose, but with anomalous lines of extinction. Supposed root contains high levels of Ca and Fe. Note also the presence silt to sand-size calcitic inclusions with high interference colours (shell, limestone, plaster and ash clast fragments). Crossed polarised light (XPL). Scale bar = 1 mm; 5d: Detail of Fig. 5c, under PPL. This shows plant root fibres and very thin and thin (pellety) organo-mineral excrements ('Maya dark earth'), which include sand and silt-size lime floor and burnt sediment clasts for example. Scale bar = 0.50 mm; 5e: Photomicrograph of M1A (Str 14, Op 13-1; west face; MG 359); lime plaster floor fragment within 'Maya dark earth'. Fragment retains example of plastered surface (arrows) and inclusion of charcoal (Ch). Tempering material include small gastropods, fossils and large example of probable conch shell (Csh). Soil is composed of fine pellets (very thin excrements) and thin to broad aggregated granular organo-mineral excrements (Ag). PPL. Scale bar = 1 mm; 5f: As Fig. 5d, under OIL. Dark grey dark earth soil pellets and granules include fine calcitic material which is often relict of fragmented lime plaster floors. Probable conch shell (Csh) is often found as temper in lime plaster floors. The presence of burnt clay (Bc – often isotropic sediment) and charcoal (Ch) may be relict of lime burning process. Scale bar = 1 mm.

sequence of lime plaster floors, with trampled occupation soils between the floors, occurs above 1.085 m asl (MG 386; Op 13-1, Str. 14) (Fig. 2b). A similar sequence begins at a depth of 1.070 m asl (MG 377 to MG 364; Op 13-2, Str. 19) (Fig. 3b–c). At both locations, the floors include very large amounts of shell temper, as well as burnt shell of presumed burnt lime origin (EDS data on various inclusions are given in online Table 5). As in the Early Classic floors, a major temper component is isotropic clasts of tidal flat sediments rich in siliceous microfossils, such as sponge spicules (M13A: Si = 23.4–29.2%; Ca = 1.04–1.35%), which occur within the weathered, but often still birefringent, lime plaster matrix (Si = 17.3–19.4% Si; Ca = 5.06–12.1). As noted above, in Op 13-1, Str. 14, it is clear that there are examples of lime floors/constructed surfaces on which small fires were lit. Detailed EDS studies of the rubefied lime plaster floor surface, its matrix and temper, and an example of Coconut Walk ware were carried out (M3A-B; Table 5; Figs. 3b–c, 4b–e). It is clear that leaching has affected the surface in M3B, having resulted in lowered interference colours in the uppermost 1–2 mm (Ca = 4.55–6.52%), whilst laterally and below (3.5–4.00 mm) there has been less decarbonation and decalcification (Ca = 6.72–15.0%). Such leaching effects have also probably affected any salt-working residues; no major concentrations of Na and Cl were observed (Na = 0.55–1.17%; 0.31–0.67% Cl, n = 5). In Op 13-2, Str. 19, however, the sampled floor sequence seems also to record occupation trample between the floors (see below), perhaps indicating domestic or multi-use activities, as indicated in Op 13-1, Str. 14.

c) Chaotically mixed ashy and burned sediment clast layers. At both Structures 14 and 19 there are >1–2 m thick layers of pink/rubefied lime plaster floors/constructed surfaces alternating with

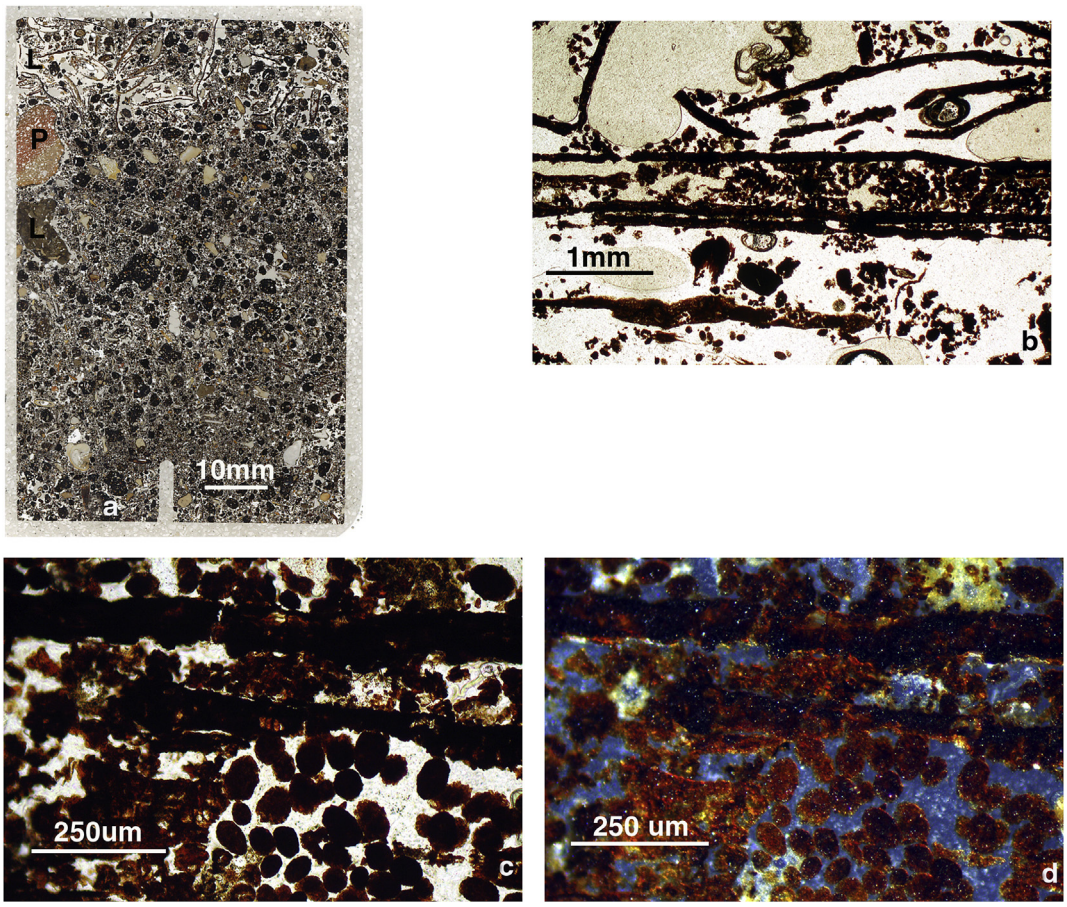

Fig. 6. 6a: Flatbed scan of MG14-M2 (surface soil with Litter layer at Str 14, Op 13-1); aggregated amorphous organic matter produced in this Litter layer forms broad excrements (black granules/crumbs) which embed fine mineral grains and remains of lime floors and shell. The Litter layer (L) is made up of leaf litter and is mixed with pellety and granular excrements. Also present are residual pot (P) and limestone/reefstone (L). Scale bar = 10 mm; 6b: Photomicrograph of MG14-M2 (surface soil with Litter layer at Str 14, Op 13-1); mainly burrowed hollow leaves partially infilled with very thin organic excrements typical of litter layers. Some residual cellular leaf material remains. Plant material has undergone both 'browning' and 'blackening' decomposition (Babel in Bullock et al., 1985). PPL, scale bar = 1 mm; 6c: As Fig. 6b. Detail of 'browned' cellular and 'blackened' plant remains and very thin oval shape organic excrements of Litter dwelling small invertebrate mesofauna. PPL. Scale bar = 250 μm; 6d: As Fig. 6c, under OIL; many plant remains and organic excrements show iron staining (chemical measurements of surface soils elsewhere found 0.85–0.92% Fe, where mercury was concentrated – 241–467 ng g^{-1} Hg). Such ferruginisation also testifies to localised and episodic hydromorphism (waterlogging). Scale bar = 250 μm.

mixed ash and burnt sediment-rich layers (see Fig. 3b–c); small amounts of iron in the isotropic clay clast temper have become rubefied and likely record low temperature (up to 4–500 °C) heating as in the Red Hills of Essex (Berna et al., 2007; Biddulph et al., 2012; Dammers and Joergensen, 1996). The deposits forming these layers are alkaline (pH 8.9) and highly saline (specific conductance [μS] of ~3000–5000), with apparently strongly enhanced high magnetic susceptibility values (see above). On the other hand, the deposits often have relatively low amounts of phosphate (unlike midden occupation floors – see below). In addition to charcoal and ash, their other chief component consists of sediment clasts. The clasts are composed of 1) calcareous and often fossil-rich sediments and 2) much higher quantities (than the calcareous sediments) of isotropic and siliceous microfossil (sponge spicule)-rich sediment materials, which, as suggested above, can be described as non-calcareous tidal flat sediments. EDS on M7B found them to be more Si-rich (Si = 19.7–21.7% Si; Ca = 1.35–3.04%) compared to calcareous sediment clast types (Si = 14.7%; Ca = 12.4%) and background ashy 'fill' (Si = 7.48%; Ca = 41.4%). When the siliceous sediment clasts include iron-staining features (Fe = 4.47–4.90%), they are markedly rubefied, which indicates subjection to heat or fire; other burnt iron-stained diatomaceous clay fragments occur within lime plaster floors. The rubefication is indicative of temperatures around 300–400 °C (Dammers and Joergensen, 1996), especially as no more strongly altered or vitrified mineral material was found at the site (Berna et al., 2007). The ubiquity of these burnt intertidal sediments is also consistent with the magnetic susceptibility and specific conductance data. As noted previously, the exposure of tidal flat sediments and the resulting concentration of salt are also probably linked to fermentation and a naturally strongly enhanced magnetic susceptibility consistent with a tropical climate; if originally calcareous these may have become decalcified and decarbonated at this time. Why is this burned sediment here, however? As a further consideration, we note that whereas most sherds from the excavations show only a loose coating of background matrix material, two large pottery fragments (quartz sand tempered Coconut Walk ware; M3A online Table 5) from processing contexts MG 374 and MG 377, retain isotropic coatings on their interiors (Fig. 4b–e). The coatings are clearly chemically different from the pot matrix. In addition these are characterised by sponge spicule microfossils and have the same chemistry as the sponge spicule-rich isotropic clay clasts found in these burnt horizons and as lime floor temper (Si = 21.3–25.5%; Ca = 1.88–7.10%; $n = 3$). Given the coring data from the 'pool' (see above) it seems likely that these coatings are formed of siliceous back-barrier mudflat sediment, which suggests an association

between the heating of the vessels and the tidal-flat sediments in the putative salt working process.

d) Trampled occupation surfaces showing minor weathering features and bone-rich midden waste. These surfaces were detected in the west face of Op 13-1 and seem to be processing debris (MG 377 within MG 832) that was either dumped, spread, or left exposed owing to a shift in the active processing locale. The deposits here are often compacted and finely fragmented, with horizontal fissuring and horizontally oriented coarse inclusions, which typifies such trampled surfaces (Cammas et al., 1996; Courty et al., 1994). The layers include shell, heated and strongly burnt bone, with much fish bone and some fine amorphous probable coprolitic fragments in places, producing marked phosphate enrichment (x5b: 18.7 mg g^{-1} phosphate-P; M13A fish bones: P = 16.1–17.1%; Ca = 37.8–39.0%; F = 0.0–2.69%; n = 4). Intact ash layers are Ca-rich and relatively P-poor (P = 0.64%; Ca = 62.2%) compared to occupation floors (P = 3.72–3.78%; Ca = 31.3–34.0%; n = 2) (online Table 5).

Of further note is the occurrence of coarse shell fragments that enclose calcitic, fossiliferous sands of presumed coral beach origin. This suggests that molluscs such as conchs were processed and then the shells dumped at site peripheries, where coral sand was washed into them; the shells were later collected for various purposes (construction, lime making) and became incorporated in occupation deposits above the beach line.

5.3. A poorly dated Late Classic or possibly later depositional sequence at Op 13-3 (Str. 8

Below the dark earth and burial-disturbed upper layers at Op 13-3 (see next section), an indurated sandy layer was recorded in the field and a sample was extracted as 'Ref 2 sand floor' (Context 385). It is composed of the following layers (Figs. 2c and 5a–b):

1. 0.42–0.41 m asl: weathered upper lime plaster floor surface,
2. 0.41–0.39 m asl: moderately intact and cemented lime plaster floor which is diffusely microlaminated ('plastered'), and with tempering composed of much bioclastic (bryozoan) reefstone, and with increased amounts of fine shell and coarse gastropod fragments, downwards; a 10 mm-size gastropod (conch?) fragment occurs, at very base of lime floor,
3. 0.39–0.37 m asl: upward-fining (coarse→medium), loose, structureless sand-size carbonate sediment rock fragments, with sand-size reefstone fossils – e.g. bryozoa – shell, including gastropods, and with shell that is often horizontally oriented. Also present is a single 8 mm-size pot fragment and few gravel-size clasts.

Archaeological context MG 385 (0.35–0.17 m asl) was assigned to sand that was detected as the highly disturbed deposit (MG 384—mixed charcoal and weathered floor material) was removed. A hard-packed surface of the sandy deposit was then detected, but the MG 385 deposit includes some admixture from beneath the sand layer. Thus the lower part of Context MG 385 as well as MG 387 are charcoal and ash-rich, with a 35 mm-thick cemented ash layer found in thin section probably comprising salt working remains. The upper part of MG 385 is distinctive, and made up of upward-fining carbonate sands, which probably record a marine inundation/beach-forming episode of diminishing energy (0.39–0.37 m asl). Both a well preserved (0.39–0.41) and a poorly preserved (0.41–0.42) lime plaster floor overlay the sand. Whatever the event (hurricane-induced sea surge?), the unheated floors overlying the sand could possibly mark a change in use of space from salt processing to domestic 'town' occupation during the Late Classic. The amount of sub-floor burials and land crab burrow-mixing material from these two periods makes such an interpretation open to question, however. Of note is that, in the field the floor overlying the sand was unrecognised until soil micromorphology was carried out.

5.4. Terminal Classic to Early Postclassic town (AD 760/800-AD 950/1000 to 1250), and Contact and Colonial Period deposit weathering and dark earth formation

Dark earth was studied from Op 13-1, 13-2, 13-3 (Strs. 14, 19, 8), including Context 379 at Op 13/3. Typical of dark earth *sensu lato* (Macphail, 1994; Nicosia et al., In press), there has been weathering and partial to total homogenization of once stratified archaeological levels, with both decarbonation and decalcifying of *in situ* 'ghosts' of lime floors for example in places – yellow brown (YB) deposits noted in the field (online Table 5). In areas of large burrows and possible burial pits no *in situ* floor remains occur (Fig. 3d). Dark Earth is a mainly blackish, humic and very fine charcoal-rich soil. It can also be coarsely mixed with another microfabric type which is dark yellowish brown because calcareous weathered plaster remains are intimately mixed with charcoal and humus; as would be expected the less Ca-rich dark humic microfabric becomes more dominant upwards (M1A-B; online Table 5; see Fig. 5c–d). Both soil microfabric types occur as 'very thin', 'thin' and 'broad' organo-mineral excrements (Bullock et al., 1985), sometimes appearing as loose granules. Residual materials ubiquitously include trace to occasional amounts of burnt and leached coprolitic bone, bryozoan-rich limestone bioclasts ('reefstone'), (conch?) shell fragments and fine to coarse relict lime floor fragments (Fig. 5e–f). Root traces and thin shelled gastropods of land snails are also present. Root traces often show weak iron-staining and one unknown root type, which is strongly birefringent (cellulose?) seems to be concentrating Fe (see below) (M1A; online Table 5; Fig. 5c–d). 'Ghost' floors often show relict subhorizontal/horizontal concentrations/layers of clay, reefstone and shell tempering that are very weakly cemented by micritic calcite remains.

Bulk soil analyses confirmed the calcareous nature of the Dark Earth (>50% carbonate), but some sample sequences show the progressive effects of leaching up-profile, for example at Op 13/3 (Str. 8), in samples 8c-8a (59.1%→54.8 → 50.5% carbonate; online Table 2). As noted at other sites where carbonate components were high but have been reduced by decarbonation (Duchaufour, 1982,74-75) more strongly residual inclusions and total phosphate can become concentrated (Crowther, 2007; Macphail, 2007). This appears to be the case with the Structure 8 sample 8c-8a sequence (3.66 → 6.26→7.25 mg g^{-1} phosphate-P; onlineTable 2). In Op 13-2 (Str. 19), pH is still alkaline, but leaching seems to have greatly reduced specific conductance some 30 cm below the modern surface soil (e.g. as low as 184 μS in sample ×12a). Soil micromorphology also shows evident mixing with the modern surface soil at Op 13/3 (Str. 8), and here Hg levels are markedly increased.

Dark earth was also characterised employing SEM/EDS studies at Op 13/1 (Str. 14), on samples M1 (dark earth peds and common but unidentified plant root example) and M1B (dark earth peds above and below lime plaster floor 'ghost'). These can be summarised as shown in the following (online Table 5):

- M1A: Calcareous yellow brown dark earth peds (mesofaunal droppings) formed from weathered anthropogenic layers are more Ca-rich (Ca = 30.4–35.3%), compared to less calcareous (decarbonated and partially decalcified) humic dark earth peds (Ca = 7.21–20.1%)

- M1A: Iron-stained fibrous root of an unknown plant seems to be concentrating Fe (Fe = 9.82–15.1%) compared to background levels in the dark earth soil (Fe = 4.45–4.63%).
- M1B: Studies of dark earth over lime floor remains found within the same lime floor, both areas of well-preserved lime plaster (Ca = 27.0–27.4%) and decarbonated and decalcified areas (Ca = 21.1–22.0%), with Ca in dark earth soil peds varying between 16.0 and 23.9%, testifying to the differing quantities of finely fragmented carbonate material within the soil.

These data indicate that decarbonisation and decalcification have affected calcareous anthropogenic materials, especially ash and lime plaster. Lime floor ghosts have a lower Ca content compared with ash (62.2–70.4% Ca) and lime floor matrix material (max. 44.4% Ca) from unweathered underlying archaeological layers. The most humic, decarbonated and decalcified dark earth peds appear to be enriched in P, Fe and S, whereas a plant root example is very noticeably rich in Fe, presumably relating to the recycling of Dark Earth soil elements, as detected by XRF analysis of the surface soil. It seems apparent that – 'Maya Dark Earth' – owing to the very high carbonate content (reefstone, lime plaster fragments, ash nodules) and relict salt processing residues – is quite different in origin and character when compared to ADE, which have a neutral to acid pH and relatively low Ca content (Arroyo-Kalin, 2010, 2014). In fact, Maya Dark Earth – as a Calcaric Brown Soils *sensu lato* – may have more in common with Roman/post-Roman European Dark Earth formed in the remains of lime-based Roman building materials (plasters and mortars), which have a high base status carbonate-rich character (Macphail, 1994; Nicosia et al., In press). In addition, terms used in European Dark Earth studies might be applicable. For example, 'pale dark earth' is used in situations in which weathered building debris dominates and only small amounts of very fine charcoal occur in the matrix soil. 'Dark Earth' proper would apply to situations in which only small amounts of anthropogenic materials remain and the earth is 'dark' owing to the very high concentrations of finely fragmented charcoal that dominate the soil matrix (Macphail and Courty, 1985).

As discussed below, the present-day surface soils – that is, the humic layer – also seem to differ from ADEs. Future studies should include the Maya Dark Earth at Colson Point, Belize, where the geology is non-calcareous (and not reefstone) (Graham, 1994) to test the rigour of the above suggestions.

That land crab action and sub-floor burial have an important role in the formation of Maya Dark Earth is more strongly indicated at Op 13-3 (than at Op 13-1 and Op 13-2) owing to their clear contribution to the homogenization process (compare Fig. 2a–c). Additional studies are essential, however. More needs to be documented concerning the history at the site of crab behaviour (for example, crab burrowing seems to be in evidence in the Terminal Preclassic deposits of Op 13-2 and in the processing deposits at all operations), and more needs to be quantified with respect to the chemical contribution of human burial to the soil. Regarding land crabs, proximity to the ground water table is likely an important factor; thus ground-raising affected the facility with which crabs could reach the water. A further complication was recognised within the dark earth of Op 13-3 (Fig. 2c), where there was evidence of *in situ* deposition of faecal waste – either of human or possibly pig origin (Macphail and Crowther, 2011; Macphail and Goldberg, 2010). This phenomenon, given where it occurred in the sequence, seems to reflect post-town Late Postclassic or later/colonial occupation (?) and an occurrence contemporary with Dark Earth formation.

Dark earth formation cannot, however, simply be dated to the decline of the town in the early 13th century, because the site experienced chronological and spatial variations in use of space in subsequent years. In addition, just as in Roman and Late Roman towns and cities, throughout the site's history there would have been areas of active processing and construction/dwelling, and others where vegetation invaded abandoned house plots, or where plots were used as midden dumps (Macphail, 1994, 2010). As indicated today by Op 13-3, areas at lower elevations would have been prone to flooding and would have been more heavily colonised by land crabs owing to the proximity of the water table.

5.5. Modern Litter (L) and surface soil (Ah1 horizon) development

Litter layers (e.g. 20 mm-thick) include horizontally oriented leaves and extremely thin organic excrements (of Oribatids?) and broad organic excrements composed of finely comminuted plant fragments (Fig. 6a–d); aggregated amorphous organic matter produced in this Litter layer forms broad excrements (granules/crumbs) which embed fine mineral grains and remains of lime floors, shell and reefstone fossils. Faunal remains include land snails. Studies of termite nest reference thin sections suggest that amorphous organic matter probably includes the remains of termite nests. Surface soils are the most organic (highest LOI at 26.9–28.0% LOI) and mercury (Hg)-rich (max 467 ng g^{-1} Hg), and least alkaline and leached layer type found at Marco Gonzalez (pH = 7.9; carbonate = 35.9%; specific conductance = 455-477 μS). It is a biologically mixed humic mineral soil and litter (L) layer of a typical broadleaved woodland (see Fig. 1c) Mull humus horizon type, which is granular to extremely fine pellety in character (Barrat, 1964). Unlike the dark earth, these surface soils and litter layers include very little fine or very fine charcoal and testify to surface accumulation and mixing of organic matter from inputs of plant litter, roots and termite nest materials, and where there has been little anthropogenic disturbance and accretion compared to Maya times. Some secondary iron impregnation features of plant and organic faecal material of mesofauna origin was also noted in thin section, consistent with XRF measurements (Fig. 6a–d). Although much residual anthropogenic material – fused ash, lime plaster, reefstone, burnt bone, pottery fragments – is present and probably contributes to some strong phosphate concentrations, its formation is in reality related to its current broadleaved caye forest vegetation cover, and thus differs from the underlying dark earth (the exact nature of the vegetation contemporary with Maya occupation and dark earth formation is still a matter speculation, but models of dark earth soil formation in Europe are based on >20 years of monitoring of post-blitz London and Berlin (Macphail, 1994). On the other hand, rooting into the archaeological levels undoubtedly has physically and chemically influenced the development of surface soil and anomalous vegetation cover. How much of an influence is dependent on many factors. For example, Hg concentrations in organic soils are naturally more enhanced from being preferentially adsorbed to organic matter compared to more minerogenic material. Whether Hg has been enriched in the surface soil by root uptake of Hg from depth requires further study, especially owing to plant species-specific differences in uptake and our spatially limited number of excavated samples; it is possible that dietary residues from consumption of large reef fish are a source that is worthy of further investigation. Although roots may contain high concentrations of Hg (reflecting soil Hg), there is often little transportation to above-ground wood and leaves (Greger et al., 2005). If low Hg concentration leaf litter is however permitted to accumulate and degrade (due to high litterfall rates, enhanced microbial activity or sheltered from disturbance) this may provide a mechanism for Hg enhancement. In addition, these surface soils often have the greatest amount of acid-insoluble quartz sand (~8–14%) compared to the underlying archaeological levels; this could in part be the result of imported quartz sand-tempered

pottery breakdown. The study of the present-day surface soil was rewarding in aiding an understanding the weathering and soil formation processes at this Dark Earth site, and future excavations could probably benefit from similar investigations.

6. Discussion and conclusions

The suite of methods was consistent with those used for studying coastal archaeological sites elsewhere. Soil micromorphology (44 thin sections) —entailing SEM/EDS – bulk soil testing for organic matter (LOI), carbonate content, salinity, fractionated phosphate and magnetic susceptibility (39 samples) and particle size analysis from three test pits and surface soils was complemented by XRF elemental analyses and cold vapour-atomic fluorescence spectrometry (CV-AFS) measurements of Hg were carried out on a parallel series of bulk samples. This permitted a fully integrated geochemical investigation. By employing all these findings and background archaeological materials recovery, it has been possible to make both detailed and broad interpretations of the sequences from the three operations (Op 13-1, 13-2 and 13-3; online Table 1). In addition, notes on charcoal analysis, the modern vegetation and soil cover, and observations on faunal activity, are included from a multi-author paper (Graham et al., 2015). Although the lower archaeological strata lay below water level, test pits and coring were able to identify ~1 m-thick infilling of low ground with ash and fine bone-rich colluvium in the Terminal Preclassic to Early Classic period (ca. A.D. 1–250). Sediment ripening and lime plaster floors were also found. Major ground raising of at least another metre occurred in Late Classic times (ca. A.D. 550/600 to 700/760), evidenced by alternating 'pink' lime floors and charcoal-rich ash layers. In these strata, lime floors – which include burned shell – were rubefied by small fires, now patchily preserved as very thin ash and charcoal layers. These lime 'floors', ash, and charcoal layers are believed to be processing remains associated with salt working. Hyposaline salt water from salt pans and/or tidal flat sediments was employed as a brine source (e.g. intact sediment coatings on vessel fragments); the brine was then gently heated over small fires. The salt-processing hypothesis is consistent with the marked presence of rubefied tidal flat sediment clasts in the burned debris layers, which exhibit a high salinity and very strongly enhanced magnetic susceptibility. Weathering effects – including rain and humic acid-associated leaching and decarbonation – exacerbated by tree root, land crab, and inhumation disturbances which can deeply penetrate the archaeological levels, have developed a specific Maya Dark Earth and modern surface soil type. Reasons why this surface soil at the three sampled profile locations is so mercury-rich are discussed. Only ghosts of lime floors remain in the archaeological levels, and occupational (e.g. burned bone, coprolitic material, conch shell) and processing (burned sediment, fused ash, pottery) debris occur within a dark humic and highly biologically worked soil. Finely fragmented charcoal originating from the Late Classic processing levels greatly contributes to the anomalous colour of the Dark Earth, probably more so than soil humus, *sensu stricto*. In this way, owing to the high carbonate contribution from the carbonate-rich lime-based floors and ash remains, the Marco Gonzalez Dark Earth ('Maya Dark Earth') differs from typical Amazonian Dark Earths. Other sites where weathered lime based building materials have been investigated using soil micromorphology (Straulino et al., 2013) have not had their associated Dark Earth deposits studied in the same way, unfortunately.

Our chief findings can be summarised (Table 1) as:

- Ash and bone-rich colluvium indicates major Terminal Preclassic occupation, although deposits so far investigated are in secondary locations. Intensive marine resource exploitation and coastal trade are indicated by faunal remains and dense sherd deposits.
- Ensuing Early Classic *in situ* occupation deposits include lime plaster floors and interbedded trampled floor deposits, with an example of an extremely bone- and phosphate-rich trampled midden layer. These contexts record the use of isotropic, sponge spicule-rich mud flat clay material as a lime plaster floor temper.
- Heated Late Classic lime plaster floors, ash and *in situ* hearth layers, and dumped highly saline (specific conductance) contexts are dominated by ash and charcoal (fuel waste), and burnt sponge spicule-rich mud flat clay clasts. Dumped deposits also contain ceramic sherds, previously implicated in salt processing (Graham, 1994: 153–156, Figs. 5.7 and 5.8) coated by the same isotropic and sponge-spicule-rich mud flat sediment found as burnt inclusions in the processing deposits. These sherds are from ceramic containers—either bowls or a basin—of a type named 'Coconut Walk unslipped', originally implicated in salt processing at the Colson Point sites along the Belize coast, in the Stann Creek District (Aimers et al., 2015; Graham, 1994: 153–156, Figs. 5.7 and 5.8). Indications are that salt working at Marco Gonzalez entailed the processing of salt-rich sediments to produce highly concentrated brine (cf. Biddulph et al., 2012). Lime, for plaster floors, seems to have been manufactured by burning shell such as conch. Domestic space was also recorded alongside kitchen middens, weathering and coprolitic inclusions (possible guano); the last may indicate the presence of birds at times, which hints that occupation was seasonal (cf. soil micromorphology of caves such as Mesolithic Uzzo Cave, Sicily; Mannino and Thomas, 2004-6).
- At Op 13-3 (Str. 8), a marine inundation event forming an upward-fining sandy (beach) sediment was recorded above salt working levels, as far as can be judged from this highly disturbed sequence. The natural sands were sealed by an unheated lime plaster floor. Clearly it will be useful to attempt to trace this sand layer outside Op 13-3.
- Deposits that reflect the various construction and occupation activities of people living in the town established at the end of the Classic period and continuing into Terminal and Early Postclassic times did not provide the detail amenable to soil micromorphological study, probably owing to the fact that they were not protected by much in the way of later construction. Skeletal remains of burials of the period, however, and burial accompaniments are generally in good condition. The deposits are broadly characterised as Maya Dark Earth where bio-working and weathering (decalcification and decarbonation) has produced very fine charcoal-rich pellety and granular soils which include weathered 'ghosts' of lime plaster floors. These deposits are still calcareous/carbonate-rich owing to the presence of these 'ghosts' and large amounts of shell, bioclastic reefstone, and ash nodules, which are relict of hearth deposits and lime floor tempers. Based on present evidence, we suggest that Dark Earth formation was not tied to any specific period in post-Late Classic times, but could have been initiated in any unoccupied space, as suggested in Roman and post-Roman European settlement use of space models.

Modern surface soils are woodland Mull humus horizons with an uppermost leaf litter layer. These differ from the underlying Maya Dark Earth and typical Amazonian Dark Earth, by being humus-rich rather than containing high amounts of very fine charcoal. The surface soils are the result of the current vegetation cover that is recycling nutrients and other elements from the underlying archaeological accumulations, including the Dark Earth. In particular, significantly elevated surface mercury concentrations adsorbed to organic matter are recorded; mercury could be

recycled from dietary residues – large reef fish. The study of the present-day surface soil at Marco Gonzalez has contributed significantly to our understanding of the weathering and soil formation processes at the site. We suggest that the study of modern-day soils should be undertaken more broadly as an excavation strategy because it provides insight into site formation processes. If Dark Earths are investigated because of their fertility, it seems logical to include the modern surface soils formed over them in any investigation, if the full potential of Dark Earths for agricultural sustainability is to be fully appreciated. In addition, the work shows that a further way of understanding how Dark Earth forms and influences the modern soil cover, is through the detailed investigation of surface soils at Maya sites. These are neo-formed through the recycling of nutrients by woodland, forming fertile soils that have been extracted for gardening on the caye. There are therefore two more areas worthy of investigation identified here.

- 1: Is the Marco Gonzalez Dark Earth unique or common to other Maya sites where lime-based constructions have decayed?, and,
- 2: leading from this, should not modern surface soils be studied alongside these Maya Dark Earths, if the true phenomenon of sustainable agriculture based upon tropical dark earths is to be better understood.

Our intention here is to demonstrate the multi-dimensional significance and expanded potential of soil micromorphological studies. At Marco Gonzalez, such studies have contributed to our understanding of the character of archaeological deposits (e.g., ghost floors, tidal clasts, working/walking surfaces reflected in microscopic trampled fish bones, fragmented charcoal, ash clasts and burned sediment). Our knowledge of the cultural significance of such deposits has also been increased, notably by the probable evidence, in the form of tidal flat sediment clasts, of salt processing. Exactly how salt was produced at the site remains to be known, but the tidal flat sediment clasts may reflect the process elucidated by McKillop (2000, 51) in which seawater is poured through salt-saturated sediment to produce an enriched brine for boiling (see also McKillop, 2015). At coastal sites excavated by McKillop in southern Belize, evidence has been recovered of brine-boiling jars and their cylindrical supports (2002, 51–52, Fig. 3.1). Similar evidence has not been recovered thus far at Marco Gonzalez, but absence may simply reflect the fact that the processing levels we have encountered contain only the debris of a final stage (McKillop, 2002, 51; Reina and Monaghan, 1981), in which salt cakes were produced by heating the enriched brine in the Coconut Walk ceramic containers. Our evidence does suggest that the friable vessels were used only once, with the vessel fragments then discarded.

The major drive behind the research focused on Marco Gonzalez, to which knowledge of the Maya cultural dimension is essential, is elucidation of the environmental impact of human activity, particularly the development of the local dark earths. Soil micromorphology has been essential in documenting the history of the deposits at the site—both natural and cultural—after they were laid down. A key finding has been the extent to which depositional elements 'migrate' and can affect surface soils (e.g. the quartz which originates as ceramic temper).

Our research will clearly benefit from more extensive excavation. The Late Classic salt-processing deposits have been exposed only in test pits. The deposits lie beneath the Terminal Classic town's structures with their multitude of burials below house floors, which in turn lie beneath a considerable spread of Post-classic material. The salt processing deposits overlie what appears to be an Early Classic settlement replete with distinctive masonry construction and with evidence of fishing and trading activities that extend back to Terminal Preclassic times. All of this activity is clearly important culturally, perhaps especially in the case of the burst of salt production that parallels Late Classic florescence on the mainland. From our point of view, however, the association of the site with Dark Earth formation provides an example in which intensive human activity can be linked to enhanced soil fertility. There is no evidence thus far from our research that intentionality was involved in dark earth formation (Graham et al., 2015), although further archaeological investigation is essential to clarify the activities represented by the charcoal layers. Nonetheless the association tells us that even inadvertent human behaviour–living, working, discarding, leaving debris, dying–can potentially affect soils positively, and this outcome has implications today both for long-term estimates of soil fertility and the decision-making involved in the contents of land fill and the future of land fill sites.

Acknowledgments

We thank Dr. John Morris and the staff of the Institute of Archaeology, National Institute of Culture and History, for granting permission to carry out the work in Belize. The multi-disciplinary undertaking in 2013 and 2014 that produced the research reported here would not have been possible without funding provided through a Research Grant (RPG-2013-204) from the Leverhulme Trust. Additional funding has been provided by the UCL Institute of Archaeology and the UCL Institute for Sustainable Research. Excavations at Marco Gonzalez in 1986 and 1990 were funded by the Social Sciences and Humanities Research Council of Canada and the Royal Ontario Museum. Graham thanks her co-PI, Scott Simmons, for kindly tolerating her divergence into soils research. We thank David Pendergast for his continued support and advice on our project and its publications, and are indebted to Jan Brown, Chairman of the Board of the Marco Gonzalez Maya Site, Ambergris Caye, Ltd., Preservation Group for all her efforts on our behalf. We thank Eduardo Barrientos and Denver Cayetano from the University of Belize and Dr. Elma Kaye, Terrestrial Science Director of the Environmental Research Institute, for their invaluable assistance, and Jerry Choco for excellent site management. Macphail gratefully acknowledges Tom Gregory and Kevin Reeves (Institute of Archaeology, University College London) for their SEM/EDS support. For supporting the ideas over the years that led to the field research, Graham would like to thank William Woods, William Balée, Eduardo Neves, Dirse Kearn, Paul Sinclair, Tim Beach, Sheryl Luzzader-Beach, and the Royal Botanic Garden Edinburgh, especially Peter Furley, Sam Bridgewater and David Harris.

Appendix A. Supplementary data

Supplementary data related to this article can be found at http://dx.doi.org/10.1016/j.jas.2016.06.003.

References

Aimers, J., Haussner, E., Farthing, D., 2015. In: Morris, J., Badillo, M., Batty, S., Thompson, G. (Eds.), The Ugly Duckling: Insights into Ancient Maya commerce and Industry from Pottery Petrography. Institute of Archaeology, National Institute of Culture and History (NICH), Belmopan, Belize, pp. 89–95.

Aimers, J., Haussner, E., Farthing, D., Murata, S., 2016. An expedient pottery Technology and its implications for ancient Maya Trade and interaction. In: Walker, D. (Ed.), Perspectives on the Ancient Maya of Chetumal Bay. University Press of Florida, Gainesville (in press).

Arroyo-Kalin, M., 2009. Steps towards an ecology of landscape: the pedo-stratigraphy of anthropogenic dark earths. In: Woods, W.I., Teixeira, W., Lehmann, J., Steiner, C., WinklerPrins, A., Rebellato, L. (Eds.), Amazonian Dark Earths: Wim Sombroek's Vision. Springer Science, New York/Berlin, pp. 99–125.

Arroyo-Kalin, M., 2010. The amazonian formative: crop domestication and anthropogenic soils. Diversity 2, 473–504.

Arroyo-Kalin, M., 2014. Amazonian Dark Earths: geoarchaeology. In: Encyclopedia

of Global Archaeology, vol. 1. Springer, New York, pp. 168–178.
Arroyo-Kalin, M., Neves, E.G., Woods, W.I., 2009. Anthropogenic dark earths of the central Amazon region: remarks on their evolution and polygenetic composition. In: Woods, W.I., Teixeira, W.G., Lehmann, J., Steiner, C., WinklerPrins, A.M.G.A., Rebellato, L. (Eds.), Amazonian Dark Earths: Wim Sombroek's Vision. Springer, London, pp. 99–125.
Avery, B.W., Bascomb, C.L., 1974. Soil Survey Laboratory Techniques. Harpenden, Soil Survey of England and Wales, Soil Survey Technical Monograph.
Ball, D.F., 1964. Loss-on-ignition as an estimate of organic matter and organic carbon in non-calcareous soils. J. Soil Sci. 15, 84–92.
Barrat, B.C., 1964. A classification of humus forms and microfabrics in temperate grasslands. J. Soil Sci. 15, 342–356.
Beach, T., Dunning, N., Luzzadder-Beach, S., Cook, D.E., Lohse, J., 2006. Impacts of the ancient Maya on soils and soil erosion in the central Maya Lowlands. Catena 65 (2), 166–178.
Beach, T., Dunning, N.P., 1995. Ancient Maya terracing and modern conservation in the Peten rain forest of Guatemala. J. Soil Water Conservation 50, 138–145.
Beach, T., Luzzadder-Beach, S., Cook, D., Dunning, N., Kennett, D.J., Krause, S., Terry, R., Trein, D., Valdez, F., 2015. Ancient Maya impacts on the Earth's surface: an Early Anthropocene analog? Quat. Sci. Rev 124, 1–30.
Beach, T., Terry, R., Brown, C., Luzzadder-Beach, S., 2009. Terra preta in Maya soils. In: Paper Presented at the Association of American Geographers Annual Meeting, Las Vegas NV, 26 March.
Bell, J., McGrath, E., Biggerstaff, A., Bates, T., Bennett, H., Marlow, J., Shaffer, M., 2015. Sediment impacts on marine sponges. Mar. Pollut. Bull. 94 (1–2), 5–13.
Berna, F., Behar, A., Shahack-Gross, R., Berg, J., Boaretto, E., Gilboa, A., Sharon, I., Shalev, S., Shilstein, S., Yahalom-Mack, N., Zorn, J.R., Weiner, S., 2007. Sediments exposed to high temperatures: reconstructing pyrotechnological processes in late bronze age and iron age strata at Tel dor (Israel). J. Archaeol. Sci. 34, 358–373.
Biddulph, E., Foreman, S., Stafford, E., Stansbie, D., Nicholson, R., 2012. London Gateway. Iron Age and Roman Salt Making in the Thames Estuary; Excavations at Stanford Wharf Nature Reserve. Oxford Archaeology, Essex. Oxford.
Boorman, L., Hazelden, J., Boorman, M., 2002. New salt marshes for old - salt marsh creation and management. In: Littoral 2002, the Changing Coast. Porto - Portugal, EUCC, pp. 35–45.
Borderie, Q., Devos, Y., Nicosia, C., Cammas, C., Macphail, R.I., 2014. Chapter 18. Dark Earth in the geoarchaeological approach to urban contexts. In: Arnaud-Fassetta, G., Carcaud, N. (Eds.), French Geoarchaeology in the 21st century. CNRS, Paris, pp. 245–258.
Bullock, P., Fedoroff, N., Jongerius, A., Stoops, G., Tursina, T., 1985. Handbook for Soil Thin Section Description. Waine Research Publications, Wolverhampton.
Cammas, C., Wattez, J., Courty, M.-A., 1996. L'enregistrement sédimentaire des modes d'occupation de l'espace. In: Castelletti, L., Cremaschi, M. (Eds.), Paleoecology; Colloquium 3 of XIII International Congress of Prehistoric and Protohistoric Sciences, vol. 3. ABACO, Forli, pp. 81–86.
Cook, D.E., Kovacevich, B., Beach, T., Bishop, R., 2006. Deciphering the inorganic chemcial record of ancient human activity using ICP-MS: a reconnaissance study of late Classic soil floors at Cancuen, Guatemala. J. Archaeol. Sci. 33 (5), 628–640.
Courty, M.A., 2001. Microfacies analysis assisting archaeological stratigraphy. In: Goldberg, P., Holliday, V.T., Ferring, C.R. (Eds.), Earth Sciences and Archaeology. Kluwer, New York, pp. 205–239.
Courty, M.A., Goldberg, P., Macphail, R.I., 1989. Soils and Micromorphology in Archaeology. Cambridge University Press, Cambridge.
Courty, M.A., Goldberg, P., Macphail, R.I., 1994. Ancient people - lifestyles and cultural patterns. In: Etchevers, J.D. (Ed.), Transactions of the 15th World Congress of Soil Science, International Society of Soil Science, Mexico, vol. 6a. International Society of Soil Science, Acapulco, pp. 250–269.
Crowther, J., 2007. Chemical and magnetic properties of soils and pit fills. In: Whittle, A. (Ed.), The Early Neolithic on the Great Hungarian Plain: Investigations of the Körös Culture Site of Ecsegfalva 23, Co. Békés, Volume I. Institute of Archaeology, Budapest, pp. 227–254.
Crowther, J., 2014. Chemistry, magnetic susceptibility and particle size of various contexts from the Marco Gonzalez Maya site, Belize. In: Graham, E. (Ed.), The Investigations at Marco Gonzalez, 2013-14, Report Submitted to the Belize Institute of Archaeology, Belmopan, Belize. Institute of Archaeology, University College London, London.
Dammers, K., Joergensen, R.G., 1996. Progressive loss of Carbon and Nitrogen from simulated daub on heating. J. Archaeol. Sci. 23, 639–648.
Dick, W.A., Tabatabai, M.A., 1977. An alkaline oxidation method for the determination of total phosphorus in soils. J. Soil Sci. Soc. Am. 41, 511–514.
Duchaufour, P., 1982. Pedology. Allen and Unwin, London.
Dunn, R.K., Mazzullo, S.J., 1993. Holocene paleocoastal reconstruction and its relationship to Marco Gonzalez, Ambergris caye, Belize. J. Field Archaeol. 20 (2), 121–131.
Gischler, E., Hudson, H.J., 2004. Holocene development of the Belize barrier reef. Sediment. Geol. 164, 223–236.
Gischler, E., Lomando, A.J., Hudson, J.H., Holmes, C.W., 2000. Last interglacial reef growth beneath Belize barrier and isolated platform reefs. Geology 28, 387–390.
Glanville-Wallis, F., 2015. 'Of Crabs and Men': Artefact Analysis of Residual Waste Deposits and a Preliminary Investigation into Crab Bioturbation at Marco Gonzalez. Belize [BSc Archaeology Dissertation]. Institute of Archaeology, University College London, London.
Glaser, B., Birk, J.J., 2012. State of the scientific knowledge on properties and genesis of Anthropogenic Dark Earths in Central Amazonia (terra preta de índio). Geochimica Cosmochimica Acta 82, 39–51.
Glaser, B., Woods, W.I. (Eds.), 2004. Amazonian Dark Earths: Explorations in Space and Time. Springer-Verlag, Berlin.
Goldberg, P., Macphail, R.I., 2006. Practical and Theoretical Geoarchaeology. Blackwell Publishing, Oxford.
Graham, E., 1994. The Highlands of the Lowlands: Environment and Archaeology in the Stann Creek District, Belize, Central America. Monographs in World Archaeology 19. Prehistory Press, Madison, Wisconsin and Royal Ontario Museum, Toronto.
Graham, E., 1998. Metaphor and metamorphism: some thoughts on environmental meta-history. In: Balée, W. (Ed.), Advances in Historical Ecology. Columbia University Press, New York, pp. 119–137.
Graham, E., 2006. A neotropical framework for *Terra Preta*. In: Balée, W., Erickson, C.L. (Eds.), Time and Complexity in Historical Ecology. Columbia University Press, New York, pp. 57–86.
Graham, E., Pendergast, D.M., 1989. Excavations at the Marco Gonzalez site, Ambergris cay, Belize, 1986. J. Field Archaeol. 16, 1–16.
Graham, E., Pendergast, D.M., 1992. Maya urbanism and ecological change. In: Steen, H.K., Tucker, R.P. (Eds.), Changing Tropical Forests. Forest History Society/Duke University Press, Durham, N.C, pp. 102–109.
Graham, E., Simmons, S.R., 2012. Ambergris Caye, Belmopan. Report on the 2010 Excavations at Marco Gonzalez, Ambergris Caye (Submitted to the Belize Institute of Archaeology, Belmopan). Institute of Archaeology, University College London, London.
Graham, E., Macphail, R.I., Turner, S., Crowther, J., Stegemann, J., Arroyo-Kalin, M., Duncan, L., Whittet, R., Rosique, C., Austin, P., 2015. The Marco Gonzalez Maya site, Ambergris Caye, Belize: assessing the impact of human activities by examining diachronic processes at the local scale. Quat. Int. xxx 1–28. http://dx.doi.org/10.1016/j.quaint.2015.08.079.
Greger, M., Wang, Y., Neuschutz, C., 2005. Absence of Hg transpiration by shoot after Hg uptake by roots of six terrestrial plant species. Environ. Pollut. 134 (2), 201–208.
Heiri, O., Lotter, A.F., Lemcke, G., 2001. Loss on ignition as a method for estimating organic and carbonate content in sediments: reproducibility and comparability of results. J. Paleolimnol. 25, 101–110.
James, N.P., Ginsburg, R.N., 1979. The Seaward Margin of Belize Barrier and Atoll Reefs. Special Publication No. 3, International Association of Sedimentologists. Blackwell Scientific, Oxford.
Lehmann, J., Kearn, D.C., Glaser, B., Woods, W.I. (Eds.), 2003. Amazonian Dark Earths: Origin, Properties, Management. Kluwer Academic, Dordrecht, Netherlands.
Macphail, R.I., 1994. The reworking of urban stratigraphy by human and natural processes. In: Hall, A.R., Kenward, H.K. (Eds.), Urban-rural Connexions: Perspectives from Environmental Archaeology, Monograph 47. Oxbow, Oxford, pp. 13–43.
Macphail, R.I., 2003. Soil microstratigraphy: a micromorphological and chemical approach. In: Cowan, C. (Ed.), Urban Development in North-west Roman Southwark Excavations 1974-90, Monograph 16. MoLAS, London, pp. 89–105.
Macphail, R.I., 2007. Soil micromorphology (chapter 11). In: Whittle, A., Kovács, G. (Eds.), The Early Neolithic on the Great Hungarian Plain: Investigations of the Körös culture Site of Ecsegfalva 23, Co. Békés. Institute of Archaeology, Budapest, pp. 189–226.
Macphail, R.I., 2010. Dark earth and insights into changing land use of urban areas. In: Speed, G., Sami, D. (Eds.), Debating Urbanism: within and beyond the Walls c. AD 300 to c. AD 700 (Conference Proceedings Leicester University Nov 15th 2008), Volume Leicester Archaeology Monograph 17: Leicester, Leicester Archaeology, pp. 145–165.
Macphail, R.I., Allen, M.J., Crowther, J., Cruise, G.M., Whittaker, J.E., 2010. Marine inundation: effects on archaeological features, materials, sediments and soils. Quat. Int. 214, 44–55.
Macphail, R.I., Courty, M.A., 1985. Interpretation and significance of urban deposits. In: Edgren, T., Jungner, H. (Eds.), Proceedings of the Third Nordic Conference on the Application of Scientific Methods in Archaeology. The Finnish Antiquarian Society, Helsinki, pp. 71–83.
Macphail, R.I., Crowther, J., 2011. Experimental Pig Husbandry: Soil Studies from West Stow Anglo-saxon Village, Suffolk, UK. Antiquity Project Gallery, vol. 85, p. 330. Antiquity. http://antiquity.ac.uk/projgall/macphail330/.
Macphail, R.I., Crowther, J., Berna, F., 2012. Soil micromorphology, microchemistry, chemistry, magnetic susceptibility and FTIR. In: Biddulph, E., Foreman, S., Stafford, E., Stansbie, D., Nicholson, R. (Eds.), London Gateway. Iron Age and Roman Salt Making in the Thames Estuary; Excavations at Stanford Wharf Nature Reserve, Essex. http://library.thehumanjourney.net/909. Oxford Archaeology Monograph No. 18, Oxford Archaeology, Oxford.
Macphail, R.I., Cruise, G.M., 2001. The soil micromorphologist as team player: a multianalytical approach to the study of European microstratigraphy. In: Goldberg, P., Holliday, V., Ferring, R. (Eds.), Earth Science and Archaeology. Kluwer Academic/Plenum Publishers, New York, pp. 241–267.
Macphail, R.I., Goldberg, P., 2010. Archaeological materials. In: Stoops, G., Marcelino, V., Mees, F. (Eds.), Interpretation of Micromorphological Features of Soils and Regoliths. Elsevier, Amsterdam, pp. 589–622.
Mannino, M.A., Thomas, K., 2004-6. New radiocarbon dates for hunter gatherers and early farmers in Sicily. Accord. Res. Pap. 10, 13–33.
McKillop, H., 2002. White Gold of the Ancient Maya. University Press of Florida,

Gainesville.
McKillop, H., 2015. In: Morris, J., Badillo, M., Batty, S., Thompson, G. (Eds.), Evaluating Ancient Maya Salt Production and the Domestic Economy: the Paynes Creek Salt Works and beyond. Institute of Archaeology, National Institute of Culture and History (NICH), Belmopan, Belize, pp. 97–105.
Nicosia, C., Devos, Y., Macphail, R.I., 2016. European 'dark earth'. In: Nicosia, C., Stoops, G. (Eds.), Encyclopedia of Archaeological Soil and Sediment Micromorphology. Blackwell, Oxford (in press).
Pendergast, D.M., Graham, E., 1987. No site too small: the ROM's Marco Gonzalez excavations in Belize. Rotunda 20 (1), 34–40.
Reina, R.E., Monaghan, J., 1981. The ways of the Maya: salt production in Sacapulas, Guatemala. Expedition 23, 13–33.
Schiffer, M.B., 1987. Formation Processes in the Archaeological Record. University of New Mexico Press, Alburquerque.
Scollar, I., Tabbagh, A., Hesse, A., Herzog, I., 1990. Archaeological Prospecting and Remote Sensing. Cambridge University Press, Cambridge.
Sombroek, W.G., 1966. Amazon Soils. A Reconnaissance of the Soils of the Brazilian Amazon Region. Centre for Agricultural Publication and Documentation, Wageningen.
Stoops, G., 2003. Guidelines for Analysis and Description of Soil and Regolith Thin Sections. Soil Science Society of America, Inc, Madison, Wisconsin.
Stoops, G., Marcelino, V., Mees, F., 2010. Interpretation of Micromorphological Features of Soils and Regoliths. Elsevier, Amsterdam.
Straulino, L., Sedov, S., Michelet, D., Balanzario, S., 2013. Weathering of carbonate materials in ancient Maya constructions (Rio Bec and Dzibanche): limestone and stucco deterioration patterns. Quat. Int 315, 87–100.
Tite, M.S., 1972. The influence of geology on the magnetic susceptibility of soils on archaeological sites. Archaeometry 14, 229–236.
Tite, M.S., Mullins, C.E., 1971. Enhancement of magnetic susceptibility of soils on archaeological sites. Archaeometry 13, 209–219.
Villaseñor, I., Graham, E., 2010. The use of volcanic materials for the manufacture of pozzolanic plasters in the Maya lowlands: a preliminary report. J. Archaeol. Sci. 37, 1339–1347.
Weiner, S., 2010. Microarchaeology. Beyond the Visible Archaeological Record. Cambridge University Press, Cambridge.
Woods, W.I., Teixeira, W., Lehmann, J., Steiner, C., WinklerPrins, A., Rebellato, L. (Eds.), 2009. Amazonian Dark Earths: Wim Sombroek's Vision. Springer, London.
Yang, H., Berry, A., Rose, N.L., Berg, T., 2009. Decline in atmospheric mercury deposition in London. J. Environ. Monit. 11, 1518–1522.